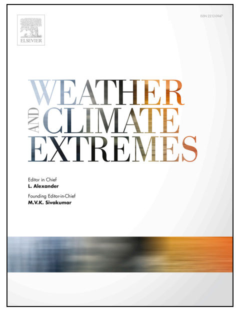

Copula-based joint modelling of extreme river temperature and low flow characteristics in the risk assessment of aquatic life

Shahid Latif, Zina Souaissi, Taha B.M.J. Ouarda, André- St-Hilaire

PII: S2212-0947(23)00039-7

DOI: https://doi.org/10.1016/j.wace.2023.100586

Reference: WACE 100586

To appear in: *Weather and Climate Extremes*

Received Date: 26 February 2023

Revised Date: 13 June 2023

Accepted Date: 13 June 2023

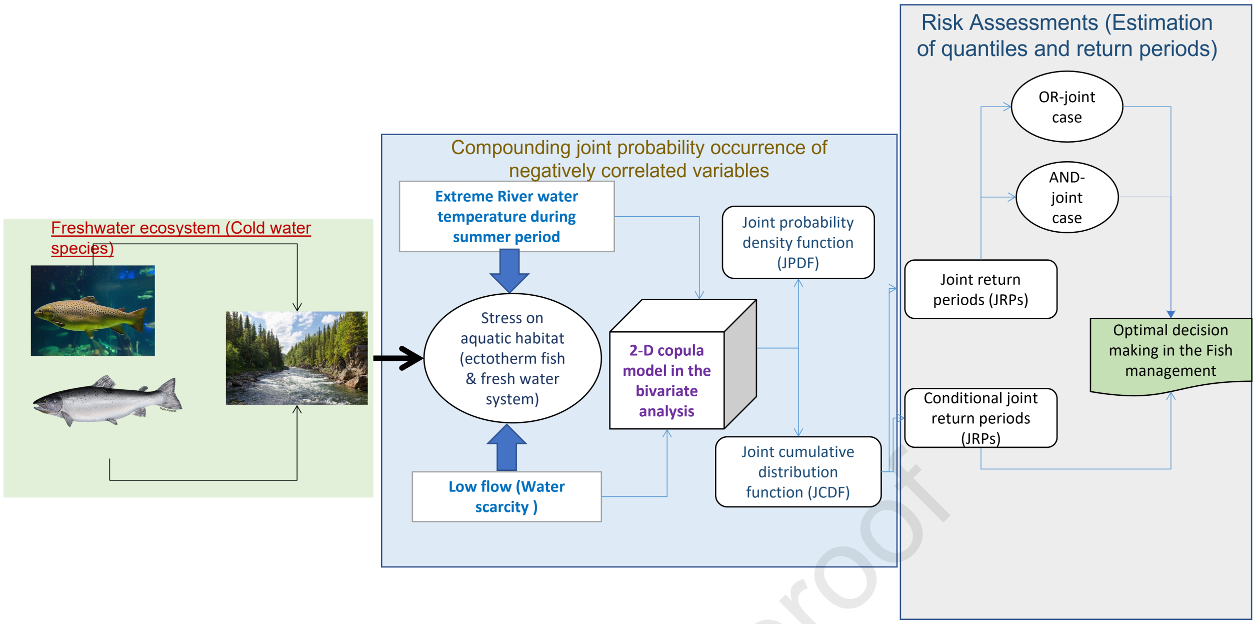
Freshwater ecosystem (Cold water species)
Compounding joint probability occurrence of negatively correlated variables
Extreme River water temperature during summer period
Stress on aquatic habitat (ectotherm fish & fresh water system)
Low flow (Water scarcity)
2-D copula model in the bivariate analysis
Joint probability density function (JPDF)
Joint cumulative distribution function (JCDF)
Risk Assessments (Estimation of quantiles and return periods)
OR-joint case
AND-joint case
Joint return periods (JRPs)
Conditional joint return periods (JRPs)
Optimal decision making in the Fish management

Copula-based joint modelling of extreme river temperature and low flow characteristics in the risk assessment of aquatic life

Shahid Latif[1*], Zina Souaissi[2], Taha B.M.J Ouarda[1], André- St-Hilaire[1]

[1]Canada Research Chair in Statistical Hydro-Climatology, Institut national de la recherche scientifique, Centre Eau Terre Environnement, INRS-ETE, 490 De la Couronne, Québec City, QC, Canada

[2] Département des Sciences de la Terre et de l'atmosphère, Université du Québec à Montréal, Pavillon Président-Kennedy, Montréal, QC H2X 3Y7, Canada

*Corresponding Author Email: Md_Shahid.LATIF@inrs.ca

Abstract

Compounding the joint impact of extreme river temperature and low flow characteristics can harm the aquatic habitat of certain organisms (e.g., ecotytherm fish) and freshwater ecosystems. Considering only river temperature or low flow via univariate frequency distribution as a stress indicator would be incomplete. Maximum water temperature and low flow series are strongly negatively correlated; thus, their joint probability distribution can be helpful to assess better the risks associated with joint extreme events. This study incorporated the 2-D parametric copulas in the bivariate joint modelling of annual maximum river water temperature and corresponding low flow. This proposed bivariate framework is applied to 5 independent and identically distributed stations in Switzerland. Parametric 1-D probability density functions are employed in modelling the univariate marginal distribution of both variables separately. The efficacy of eighteen different parametric class negatively dependent 2-D copulas is tested. The best-fitted copulas and selected marginals are used to estimate joint return periods for quantiles corresponding to multiple return periods. The joint return periods of annual maximum temperatures conditional to low flows or vice versa are also estimated. Investigation reveals that the occurrence of bivariate events simultaneously is less frequent in the AND-joint case than in the OR-joint event case for all stations. Also, OR-return periods are less (nearly half) the value of univariate return periods. Secondly, higher conditional return periods are observed in annual maximum temperature (or low flow) when increasing the percentile value of the conditioning variable, i.e., low flow (or maximum temperature). Also, when the low flow (or water temperature) conditioning variable is fixed, higher bivariate event return periods are observed at a higher water temperature (or low flow) value. In conclusion, these estimated bivariate statistics can help provide a more complete picture for an adequate assessment of the risks associated with cold-water species.

Keywords:

Switzerland, Extreme River temperature, Low flow, Copula function, Bivariate joint analysis, Joint return period, Conditional joint return period

1. Introduction

A warming climate is expected to increase rivers' mean and maximum temperatures worldwide (Boyer et al., 2021; Wanders et al., 2019 and references therein). A river's temperature is considered a highly sensitive and vital variable affecting a flowing river's physical, chemical, and biological processes (Hannah et al., 2008). It significantly impacts water quality and aquatic ecosystems' health (Caissie, 2006; Petts, 2000). River temperatures increase result in decreased dissolved oxygen concentration and a greater rate of biochemical reactions (Ficklin et al., 2013; Sand-Jensen et al., 2005). Therefore, most aquatic organisms have a specific range of temperatures that they can tolerate. In addition, high water temperatures can damage fisheries' resources by limiting their habitat or even leading to fish mortality (Caissie et al., 2007; Elliott and Hurley, 2001; Lund et al., 2002; Sundt-Hansen et al., 2018 and references therein). As an example, in the case of salmonids, an ideal temperature for juvenile Atlantic salmon (*Salmo salar*) to grow is 16-20°C (Elliott and Elliott, 2010), and higher temperatures have been found for their fish physiology and behaviour (Breau et al., 2007; Lund et al., 2002). According to Elliott and Hurley (2001), brown trout (*Salmo trutta*) grow optimally at 13.1-13.9°C, whereas growth ceases below 2.9-3.6°C and above 18.7-19.5°C. Water temperature above 19℃ can also influence vitellogenin (Vtg) concentration in brown trout's plasma (Korner et al., 2008). Temperatures above 15℃ can increase the risk of proliferative kidney disease (PKD) in brown trout populations (Strepparava et al., 2018). Thus, the characterization of the hydrological regime of rivers is essential for assessing the health of aquatic habitats.

Also, several studies have shown that water scarcity can negatively impact fish habitats and marine life, especially during low water periods. For example, water extraction can affect a river's ability to dilute contaminants and its thermal regime (Caissie, 2006). The decrease in river flows can be an ecologically stressful event likely to be exacerbated by potential climate change and other anthropogenic changes (Daigle et al., 2011). The reduction in flow may also contribute to habitat disconnectivity (Fullerton et al., 2010) and changes in river water temperature (Humphries and Baldwin, 2003; Sinokrot and Gulliver, 2000; Doug and Amy, 2021). Thus, their combined action can be more harmful and affect the water habitats. There have been several studies in the literature that have focused on the prediction of extreme river temperatures and low flows on a univariate basis (Souaissi et al., 2023; Ouarda et al., 2022; Abidi et al., 2022; Alobaidi et al., 2021; St-Hilaire et al., 2021; Souaissi et al., 2021; Caissie et al., 2020; Charron et al., 2019; Ouarda et al., 2018; Lee et al., 2017; Joshi et al., 2016; Joshi et al., 2013; St-Hilaire et al., 2012; Daigle et al., 2011; Ouarda et al., 2008; Hamza et al., 2001; Durrans et al., 1999). In bivariate frequency analysis (FA), several studies have concluded that single-variable hydrological FA provides a limited assessment of extreme events (Lee et al., 2013; Salvadori et al., 2007; Yue et al., 2001). Generally, univariate FA and their associated return periods cannot provide a complete evaluation of the probability of occurrence if correlated random variables describe the underlying event of interest. A better understanding of the phenomenon can be gained by studying the probabilistic characteristics of such events in conjunction with their joint distribution. Univariate FA is helpful when only one random variable is significant for design purposes or if the two are not strongly (and significantly) correlated (Graler et al., 2013, Reddy and Ganguli, 201; Karmakar and Simonovic, 2009). However, a separate analysis of the random variables cannot reveal their significant relationship if the correlation is essential information in the design criteria. As a result, it has been demonstrated in recent years that extreme hydrological events can be characterized by the joint behaviour of several dependent variables (Latif and Simonovic, 2022a; Latif and Mustafa, 2020, 2021; Santhosh and Srinivas, 2013; Chebana and Ouarda, 2009; Yue 2001). The multivariate FA framework is widely accepted, such as modelling flood volume, peak and duration (Fan et al., 2016; Chebana and Ouarda, 2009; Zhang and Singh, 2006); drought magnitude (De Michele et al., 2013; Kao & Govindaraju, 2010; Shiau 2006), rainfall characteristics (Salvadori and De Michele 2006), joint modelling of storm surge, rainfall, and river discharge (Latif and Simonovic 2022b, 2022c). However, only one publication estimates extremes in the thermal regime of rivers using a multivariate FA approach. Seo et al. (2022) recently focused on analyzing the effect of drought on water temperature from a probabilistic point of view using the notion of a copula distribution framework. Different correlated components can characterize extreme water temperatures.

Earlier studies incorporated different conventional parametric distributions in the bivariate and a few trivariate joint frameworks. For instance, Goel (1998) (bivariate normal model), Yue (1999) (bivariate generalized extreme value model), Yue (2000) (bivariate Gumbel model), Escalante and Raynal (1998, 2008) (trivariate Gumbel distribution) and references therein. All such conventional distributions have some statistical constraints and limitations (refer to Joe, 1997 and Nelsen, 2006 for extended details). Recently, the copula functions have been recognized as a highly flexible multivariate joint distribution tool (De Michele and Salvadori, 2003; Grimaldi and Serinaldi, 2006; Zhang and Singh, 2007; Salvadori et al., 2007; Salvadori and De Michele, 2010; Latif and Simonovic 2022a, 2022b, and references therein). The copula function allows the separate modelling of univariate marginal distributions and their joint structure, which are not necessarily from the same distribution families. The copula is frequently applied in most literature for bivariate joint distribution cases. Very few pieces of literature attempted to model the trivariate joint case of extreme events. Our study is limited to developing the 2-D copula distribution framework because of input bivariate random observations.

A period of high temperatures and low flows can increase stress for many aquatic species. In order to understand the combined action of rivers' thermal and flow regimes, multivariate joint probability distribution approaches should be adopted in the evaluation of joint exceedance probabilities and associated multivariate joint and conditional return periods; otherwise, the univariate approach might result in underestimation or overestimation of risk. This can model the actual risk associated with the joint occurrence of high river temperatures and corresponding low flow events. Previous studies used a univariate probability framework to consider only the river temperature to indicate thermal stress indicators for aquatic species at the same river stations (Souaissi et al., 2021). As far as the authors are aware, there has been no detailed analysis of the joint and conditional probability relationship between these variables for aquatic species in the Swiss River using a bivariate joint dependence framework. As a result, the novelty of this present work performed the joint distribution relationship and bivariate FA of the maximum river temperature and corresponding low flow using a parametric copula distribution framework. This study uses the joint and conditional joint probability framework and its associated exceedance probabilities for river water temperature and corresponding low flow to investigate their joint stress for aquatic habitats in Switzerland's multiple independent and identically distributed (i.i.d) stations. The objective of this present study is (1) to test the efficacy of 2-D parametric copula in the bivariate joint modelling of river water temperature and low flow characteristics; (2) to estimate bivariate primary joint return periods for both OR- and AND- joint cases and its comparison with univariate return periods; (3) to estimate conditional joint return periods of river water temperature (or corresponding low flow) given various percentile values or conditioning to low flow series (or river water temperature).

The organization of this manuscript is as follows: Section 2 presents the theoretical research framework or methodology in fitting 2-D parametric class copula functions, their dependence parameter estimations and the goodness-of-fit (GOF) test in the bivariate joint analysis. This section also presented the theoretical background of risk evaluation by estimating bivariate joint and conditional joint return periods. Section 3 presents the study area details, delineation of bivariate extreme observations, and modelling of the univariate marginal distribution of the selected variable of interest. Section 4 provides the results and discussions, selecting the most parsimonious 2-D copulas in the bivariate joint simulation, their associated primary joint return periods, and the conditional joint return periods. Lastly, Section 5 presents the research conclusions and future works.

2. Theoretical Research Framework

2.1. Bivariate dependence via parametric 2-D copula

Investigating the joint exceedance probabilities and their associated return period between river water temperature and low flow series can better understand their collective impact on aquatic habitats or fish life cycles. Figure 1 illustrates the methodological workflow model adopted in this study. Our present methodology introduced a parametric-based multivariate probabilistic framework that investigates the compound effect of river water temperature and corresponding low flow in the context of joint and conditional joint probability distribution and its associated return periods.

Insert Figure 1

Compared to the conventional multivariate models, the copula function can form the basis for estimating various quantities, which can be very useful for risk analysis, for instance, the estimation of joint and conditional joint return periods (Salvadori 2004; Shiau 2006; Salvadori and De Michele 2004). Saklar (1959) first developed the idea of the copula function. Copula connects univariate marginal distributions of multiple individual variables into multivariate joint distribution (Nelsen 2006; Salvadori and De Michele 2004). Copulas can model a wider extent of both linear and nonlinear dependencies.

If (A, B) is the bivariate random pair (historical observations), with $u = F_A(a) = P(a \leq A)$ and $v = F_B(b) = P(b \leq B)$ are the continuous univariate marginal distributions, then there is a copula dependence function 'C', which can be defined on the unit square is estimated by

$$H_{A,B}(a, b) = C[F_A(a), F_B(b)] = C(u, v) \quad (1)$$

where C is any copula function under consideration. $F_A(a)$ and $F_B(b)$ are the univariate marginal cumulative distribution functions (CDFs) of the fitted random variables A and B. $H_{A,B}(a, b)$ is the bivariate joint cumulative distribution function (JCDF) which can be defined using the bivariate copula density. Also, If the given univariate marginal distributions, $F_A(a)$ and $F_B(b)$ are continuous, then the fitted Copula must be unique (Zhang and Singh 2006). Similarly, the joint probability density of the two random characteristics, with $f_A(a)$ and $f_B(b)$ are the univariate probability density function (PDF), is estimated by

$$f_{A\,B}(ab) = c\left(F_A(a), F_B(b)\right) * f_A(a) * f_B(b) \quad (2)$$

Where c is the density function of 2-D Copula.

$$c(u, v) = \frac{\partial^2 c(u,v)}{\partial u\, \partial v} \quad (3)$$

where $u = F_A(a) = P(a \leq A)$ and $v = F_B(b) = P(b \leq B)$

Before selecting copulas as a candidate model in testing and establishing bivariate joint dependency, we confirmed that the river water temperature and the corresponding low flow exhibit negative dependency. We already measured the dependency strength between the targeted variable in section 4.2. Taking this into consideration, our present study selected and tested the efficacy of different negative dependence copula classes ($-\infty < \theta \leq 0$; θ is the copula dependence parameter). For instance, monoparametric Archimededean copulas (i.e., Frank), bi-parametric or mixed Archimedean copulas (i.e., BB1 (mixture of Clayton-Gumbel), BB6 (mixture of Joe-Gumbel), BB7 (mixture of Clayton-Joe) and BB8 (mixture of Frank and Joe)), rotated variants of Archimedean copulas (i.e., rotated Clayton, Gumbel, Clayton (each by 90 degrees)), rotated version of mixed Archimedean copulas (i.e., rotated BB1, BB6, BB7, BB8 (each by 90 degrees and 270 degrees)), one Elliptical Copula (for instance, Gaussian or Normal) (Joe 1997; Constantino et al., 2008; Manner 2010; Li et al. 2016; Tang et al. 2015; Zhang et al. 2016).

The Archimedean class copulas are highly flexible, less complex and easy to fit. For instance, Frank copula can accommodate the entire range of mutual concurrency, $\tau_\theta \in [1, -1]$. However, it can fail to capture extreme tail dependence behaviour or have a symmetrical dependence structure. Besides this, the Clayton, Gumbel and Joe copulas only exhibited positive range dependency. However, by 90 degrees, their rotated version can easily model the negatively dependent pairs and thus be employed in this study.

The bivariate Archimedean class copula is mathematically expressed as (Nelsen 2006)

$$C(u. v) = \phi^{-1}\left(\phi(u) + \phi(v)\right); \qquad \text{for } u, v \in [0, 1] \quad (4)$$

In the above Equation (4), $\phi(\cdot)$ and $\phi^{-1}(\cdot)$ are the Archimedean Copula's generator functions and their inverse. Also, the efficacy of the Gaussian (or Normal) Copula is tested in the bivariate joint analysis, and which is estimated by

$$C_\theta(u,v) = \Phi_\theta\left(\Phi_\theta^{-1}(u), \Phi_\theta^{-1}(v)\right) = \frac{1}{2\pi\sqrt{1-\theta^2}} \int_{-\infty}^{\Phi_\theta^{-1}(u)} \int_{-\infty}^{\Phi_\theta^{-1}(v)} e^{\left(\frac{-(s^2-2\theta st+t^2)}{2(1-\theta^2)}\right)} dsdt \qquad (5)$$

In Equation (5), Φ_θ is the bivariate normal CDF; Φ and Φ^{-1} are the standard normal CDF and its inverse function. The Gaussian Copula exhibits symmetric tail behaviour, unable to capture extreme tail dependence or asymptotic independence, and it is surrounded mainly by the centre or mid-range of distribution (MacNeil et al., 2005; AghaKouchak et al., 2012; Alina, 2018; Zhang et al., 2016).

On the other side, two-parameter mixture Archimedean copulas, for instance, BB1, BB6, BB7 and BB8, are highly efficient in capturing joint dependence behaviour (Joe and Hu 1996; Joe 1997; Nikoloulopoulos 2012). Such as, BB1 and BB7 can accommodate both the lower and upper tail dependence, BB6 can capture upper tail behaviour while BB8 has no tail dependencies (Joe 1997). This study also tested the adequacy of the rotational variants of the mixture Archimedean Copula by 90 and 270 degrees, which can effectively capture negative correlation behaviour. Besides this, the rotational variants of extreme value class Tawn type 1 copula (by 90 degrees) are also incorporated (Tawn 1988). All the selected candidate copula models are fitted to historical bivariate random pairs in the next following section, 2.2. Table 1 lists the mathematical description and their associated statistical properties of 2-D copulas used in this study. Readers are advised to follow 'The International Association of Hydrological and Sciences (IAHS)' for extended details and a list of copula's model applicability in hydrometeorological characteristics

Insert Table 1

2.2. Estimation of copula dependence parameters

Existing literature pointed out a different approach in the estimation of the vector of unknown statistical parameters, called copula dependence parameter(s), for instance, canonical maximum likelihood (CML), inference functions for marginal (IMF), rank-based method of moment (MOM.), exact maximum likelihood (EML) etc., (Genest and Rivest 1993; Genest et al. 1995; Joe 1997, and references therein). This study incorporated a maximum pseudo-likelihood (MPL) estimator in estimating the dependence parameters of the fitted 2-D models (Klein et al., 2010; Kojadinovic and Yan, 2010; Reddy and Ganguli, 2012). The MPL estimators utilize rank-based empirical distribution in estimating copula parameters independently from their univariate marginal distributions. The MPL is working on maximizing the pseudo-log-likelihood function $l(\theta)$ in estimating dependence parameters as given below:

$$l(\theta) = \sum_{k=i}^{m} \log\left[c_\theta\left\{F_1(X_{k,1}), F_1(X_{k,2})\right\}\right] \qquad (6)$$

In Equation (6), θ defines the copula dependence parameter; m is the random pairs size (or length) $F_1(X_{k,1})$ and $F_1(X_{k,2})$ are the empirical cumulative distribution functions (CDFs); $l(\theta)$ defines the pseudo-log-likelihood function.

2.3. Compatibility test for fitted bivariate copula model

The efficacy of the fitted candidate 2-D copula models for each station is examined using the Cramer-von Mises (CvM) test statistics. The CvM test statistics evaluate the performance of hypothesized 2-D model fitted to given bivariate random observations that make the use of Cramer-von Mises functional statistics $'S_n'$ with the parametric bootstrapping procedure (Genest and Remillard, 2008; Tosunglou and Kisi 2016) is estimated by

$$S_n = \sum_{i=1}^{n} \left\{c_n\left(U_{i,n}, V_{i,n}\right) - C_\theta(U_{i,n}, V_{i,n})\right\}^2 \qquad (7)$$

In Equation (7), $'c_n'$ is the empirical Copula estimated using the n observational random pairs; $'C_\theta'$ is the parametric 2-D Copula estimated under the null hypothesis. Besides this, the p-value of each candidate 2-D Copula (corresponding to above S_n test) is estimated using parametric bootstrapping by

$$\mathrm{p} = \frac{1}{\mathrm{N}} 1(\mathrm{S}_{\mathrm{n,t}} \geq \mathrm{S}_{\mathrm{n}}) \tag{8}$$

In Equation (8), N is the number of simulations. In conclusion, the acceptance and rejection of the candidate 2-D model are based on the fact that if the estimated p-value is larger than 0.05 (at a 5% significance level), the selected Copula must be performed satisfactorily; otherwise, liable for rejection. Also, the minimum value of the $'S_n'$ statistics (refer to Equation (7)) must indicate the most parsimonious Copula, which has minimum dispensary with the empirical Copula. This study used the free R software (R Core Team 2021) with libraries (Copula, Vine Copula and VC2copula) to compute the S_n (with parametric bootstrapping) statistics and their associated p-value (along with copula dependence parameters) for each fitted 2-D Copula.

2.4. Multivariate Risk Evaluation

2.4.1. Derivation of primary joint return periods from the bivariate distribution of extreme pairs

This study aims to investigate the joint probability occurrence of river water temperature and corresponding low flow that can adversely affect the environment and aquatic life if they occur concomitantly. Estimating design variable quantiles under different notations of return periods is essential in risk assessments of extreme events. For instance, return periods are calculated based on joint probability distribution and conditional joint probability relationship (Salvadori, 2004; Zhang and Singh, 2006; Graler et al., 2013; Serinaldi, 2015, and references therein). Different return periods estimation approaches have their importance, which cannot be interchanged and could solely depend upon the nature of the problem undertaken. This section describes the estimation of primary joint return periods for both OR- and AND-joint cases.

The joint probability relationship of river water temperature and corresponding low flow series is described in two different ways:

Case-1: when both variables exceed a particular threshold value simultaneously (say, $A \geq a$ AND $B \geq b$) and thus their associated return period, called AND-joint return period, is given by

$$\mathrm{T}^{\mathrm{AND}} = \frac{\mu}{1-\mathrm{F(a)}-\mathrm{F(b)}-\mathrm{C(F(a),F(b))}} = \frac{1}{1-\mathrm{F(a)}-\mathrm{F(b)}-\mathrm{C(F(a),F(b))}} \tag{9}$$

In Equation (9), $\mathrm{F(a)}$ and $\mathrm{F(b)}$ are the univariate marginal CDFs; $\mathrm{C(F(a), F(b))}$ is the copula-based joint CDF; μ is the average inter-arrival time between two successive occurrences of extreme events. The value of μ equals 1 when considering the extreme events at an annual scale (i.e., one event per year or annual maxima extreme value sample group) (Yue and Rasmussen 2002). The non-exceedance probabilities in the simultaneous occurrence of both events are defined by the denominator term (F(a) + F(b) - C(F(a), F(b))). of Equation (9).

Case-2: when either of the variables exceeds a particular threshold value (say, $A \geq a$ OR $B \geq b$) and thus their associated return periods, called OR-joint return periods, are given by

$$\mathrm{T}^{\mathrm{OR}} = \frac{1}{1-\mathrm{F(a)}-\mathrm{F(b)}-\mathrm{C(F(a),F(b))}} \tag{10}$$

In conclusion, Equations (9) and (10) are used in estimating joint return periods for the different possible combinations of bivariate random pairs.

2.4.2. Derivation of return periods from the conditional joint probability distribution

In examining the mutual concurrency between river water temperature and corresponding low flow characteristics, it must also be demanding to investigate the conditional joint probability relationship. In actuality, the conditional return period relies on the conditional joint probability between the variable of interest, given that some condition is fulfilled (Shiau, 2006; Zhang and Singh, 2006; Salvadori and De Michele, 2010; Sraj et al., 2014; Zhang et al., 2016 and references therein). For instance, the variation in the first variable's return periods given various percentile values of the second variable (or vice-versa).

The best-fitted 2-D Copulas, selected in previous section 2.3, are now employed in deriving the conditional probability distribution and, in further the conditional return periods, are estimated for two different bivariate cases, given by

Case 1:

$$\mathrm{T}_{\mathrm{A|B>b}} = \frac{1}{(1-\mathrm{F(b)}*(1-\mathrm{F(a)}-\mathrm{F(b)}+\mathrm{C(F(a),F(b))}} \quad (11)$$

And,

Case 2:

$$\mathrm{T}_{\mathrm{A|B\leq b}} = \frac{1}{(1-\frac{\mathrm{C(F(a),F(b))}}{\mathrm{F(b)}})} \quad (12)$$

Equations (11) and (12) indicate the conditional return period, say variable A (e.g., river water temperature), given various percentile values of the second variable, say B (e.g., corresponding low flow) or vice-versa.

3. Application

3.1. Details of the study area

The network of water temperature stations in Switzerland is chosen as a case study for this work. Figure 2 illustrates the location of the gauging stations selected for this study. The catchment areas for the five stations employed vary from a minimum of 314 km^2 to a maximum of 6299 km^2, with an average watershed elevation varying between 502 m to 1833 m. The stations selected are located at low altitudes. Relatively heavy rainfalls characterize the lower part of the country. In terms of flow, the annual cycle is moderate, with a minimum in summer, and shows a high level of interannual variability, depending on regional precipitation patterns (Michel et al., 2020). Because of Switzerland's relatively high orography, there is a fast change from liquid to solid precipitation, even on a small spatial scale.

Insert Figure 2

3.2. Delineation of the extreme bivariate observations

The traditional approach in frequency analysis or joint modelling is often employed either via block annual maxima (AM) or peak over the threshold (POT) on the partial series of data with a statistical assumption of independent and identical distribution (i.i.d) (Hosking et al., 1985; Bras 1990). The AM sampling procedure is widely accepted in most existing flood, drought or rainfall modelling applications where the sampling time interval is usually one year.

The Swiss Federal Office for the Environment (FOEN) provided the daily river water temperature and low flow dataset for different independently and identically distributed (i.i.d) stations. Both datasets have been recorded since the 1960s. This study targeted five stations with long-term records, which usually vary from 36 to 53 years (refer to the study area map, Figure 2). Flow records are available for a significant period at most stations, whereas temperature records are relatively short at most stations. Our present study selected five out of 24 stations used in the previous study by Souaissi et al. (2021). Only this selected station exhibited a significant correlation and thus can be employed in the bivariate joint modelling. This study adopted an AM sampling procedure in the extraction of the variable of interest, using the following steps

1. First, the annual maximum river water temperature data for each selected station are extracted from their maximum daily records during the summer period, from May 1 to October 31.

2. The second variable, low flow series, is defined by taking their value on the same calendar date as the annual maximum water temperature value.

Supplementary Tables (ST 1a-e) list each station's descriptive statistics of the targeted extreme random pair. Supplementary Figures (ST 1a, b) illustrate the box-whisker plots for both variables. Similarly, Supplementary Figures (SF 2a-j) show the station-wise normal quantile-quantile (Q-Q) plots which indicate the deviation of the given random observations from normality. Supplementary Figures (SF 3a-e) visualize each station's time-series behaviour of the variable of interest. Besides this, the analytical-based nonparametric Mann-Kendall (M-K) test is calculated to visualize monotonic time-trend under the null hypothesis H_0 against their alternative hypothesis H_a (refer to Supplementary Table (ST 2) (Mann 1945; Kendall 1975). In this test, the null hypothesis is accepted for all the selected stations, except for stations 2044 and 2084, where the annual maximum temperature series exhibits a positive trend or nonstationary because its calculated Z-statistics exceed the critical z-value = ±1.96 at a 5% significance level or 95% confidence interval. In conclusion, these results confirmed and supported visual inspection results.

The Ljung-Box (1978) hypothesis testing, also called Q-statistics, is estimated to investigate the existence of autocorrelation (or serial correlation) within individual time series. Under the null hypothesis H_o (zero autocorrelation) against alternative hypothesis H_a (serially correlated), Q-statistics usually follow a chi-square distribution having 'h' degrees of freedom (Daneshkhan et al., 2016). Supplementary Table (ST 3) listed the estimated Q-statistics for different lag sizes (30, 20, 10 and 5). For all the selected stations, the null hypothesis is accepted at a 5% significance level (or 95% confidence interval) for both variables, indicating no serial correlation exhibited within the historical time series. Supplementary Figures (SF 4a-e) illustrate the autocorrelation function (ACF) plots which support the analytical results.

Besides this, the homogeneity test for the given time series is performed using the Pettitt test (Pettitt 1979) and the Buishand range test (Buishand 1982), refer to Supplementary Table (ST4). This test examined if there is a time when changes occurred within individual time series. Results found that only the annual maximum temperature variable for station 2044 is not homogenous; the estimated p-value is less than 0.05 (measured at a 5% significance level). In conclusion, the above-estimated results confirmed that the annual maximum temperature for stations 2044 and 2084 exhibits time-varying behaviour or nonstationarity.

The present study did not consider the accountability of time-varying scenarios in modelling univariate marginals or their mutual dependence. It is essential to reflect the impact of climate change, anthropogenic land use activities or any other suitable external covariates in the estimated multivariate joint exceedance probabilities or return periods. Many previous studies have already pointed out the necessity of considering dynamic univariate or multivariate frameworks in the evaluation of hydrologic risk (Milley 2008; El Adlouni et al. 2007; Villarini et al. 2010; Lopez and Frances 2013; Lima et al. 2015; Chebana and Ouarda 2021 and references therein). The impact of climate change may alter river water temperature by reducing river water flow by increasing evaporation or lesser rainfall events. Also, the river water temperature can alter when there is an increased demand for water, for instance, irrigation or in municipal supply. The present study considers a stationary-based multivariate framework. Future work within our group will consider a dynamic (i.e., nonstationary) framework.

3.3. Univariate marginal probability distribution of extreme characteristics

3.3.1. Empirical univariate non-exceedance probabilities

Approximating a suitable univariate marginal probability distribution is mandatory before introducing random variables into the multivariate joint probability framework. However, copula already facilitates the selection of any best-fitted univariate margins without restriction on their family or any fixed distributions. The compatibility of the candidate model fitted to historical data is examined by comparing theoretical and empirical observations. In this study, the empirical non-exceedance probabilities, or cumulative distribution function (CDF), $P(A \leq a)$, of each target variable, are estimated using the Gringgorten-based position-plotting approach (Gringorten 1963) is calculated by

$$\text{Empirical non} - \text{exceedance probabilities} = \mathrm{P}(\mathrm{A} \leq \mathrm{a}) = \frac{(\mathrm{a}-0.44)}{(\mathrm{N}+0.12)} \quad (13)$$

In Equation (13), N is the observation sample size; a is the ath observations in the given dataset, which are arranged in ascending order. Finally, each variable's empirical CDF is compared with the theoretical CDF of the fitted candidate model to observe the gaps and dispensary between them and select the best-fitted marginal distribution using different goodness-of-fit (GOF) measures.

3.3.2. Fitting 1-D parametric distributions and their fitness investigation in defining univariate marginal structure

This study selected various parametric family-based probability functions as candidate models in defining the most justifiable univariate marginal distribution of the annual maximum temperature and corresponding low flow series for each station chosen separately. Candidate distributions include the 2-parameter Normal (Yue 1999), 2-parameter with upper bounded tailed Weibull (Johnson 1994), 2-parameter Gamma (Yevjevich 1972), 2-parameters Logistic (Bobee and Ashkar 1989), 2-parameter Lognormal (Yue 2000), 2-parameter Gumbel (Khaliq et al., 2006; Graler et al., 2013) and 3-parameters Generalized extreme value distribution (GEV) (Yue and Wang 2004). No universal rules or existing literature suggests selecting any specific or fixed distribution function family. Each selected variable would follow a different distribution and need to be modelled separately without any prior distributional assumption (Adamowski 1985, 2000). Also, different fitted probability density functions (PDF) can result in different estimations of design quantiles. For instance, the Gumbel model is characterized by a light-tailed, while the Weibull model exhibited bounded upper-tail behaviour. Supplementary Table (ST5) lists the fitted univariate models' mathematical descriptions (pdf).

The vector of unknown statistical parameters of the fitted models is estimated using the maximum likelihood estimation (MLE) (Owen 2008). The MLE algorithm can provide minimum sampling variance of the estimated distribution parameters (or estimated quantiles) (Can and Tosunglou 2013).

Selecting a suitable model to describe marginal behaviour is often challenging and demands higher accuracy through quantitative and qualitative model compatibility investigation. This study adopted different GOF test statistics, based on distance criteria statistics, called the Kolmogorov-Smirnov (or K-S) test (i.e., Xu et al., 2015) and Anderson-Darling (or A-D) test (i.e., Anderson and Darling 1954). For instance, K-S statistics is an empirical distribution function (EDF) that can investigate the largest vertices. However, the K-S statistics are characterized by relatively flat-tail distributions for both the theoretical and empirical probabilities. Thus, a quadratic class EDF is also adopted to deal with this issue, the A-D statistics. The A-D statistics can put extra weight on the tail portion and have better sensitivity near the distribution tail relative to the distribution's centre portion (Farrel and Stewart, 2006; Alam et al., 2018). Besides this, the Cramer-von Mises (CvM) statistics are also estimated with K-S and A-D tests to reveal a justifiable selection procedure (Cramer 1928; von Mises 1928). The CvM statistics is the generalization of the A-D test, an assessment of the minimum distance between the theoretical and empirical probability distribution. Hence, the minimum value of estimated K-S, A-D and CvM test statistics can result in a better fit, or the fitted model is closer to generating the original historical observations.

4. Results and Discussions

4.1. Modelling marginal distributions of annual maximum river temperature and corresponding low flow

Supplementary Tables (ST 6a-j) list the fitted 1-D candidate models using the MLE approach (refer to section 3.3.2). The fitness level of the candidate model for each variable of interest is investigated using the K-S, A-D and CvM test statistics by comparing the empirical and theoretical (or fitted model) probabilities. These quantitative GOF test measures are listed in the same tables (ST 6a-j). The results are summarized below

1. The 2-parameter Logistic distribution is identified as best-fitted in describing marginal distributions of the annual maximum temperature and their corresponding low flow series for station 2044 (minimum K-S, A-D and CvM test value compared with other peer models).
2. The 2-parameter Normal and 2-parameter Lognormal distribution performed satisfactorily in describing the marginal distribution of the annual maximum temperature and the corresponding low flow for station 2084.
3. The 2-parameter Logistic and 2-parameter Gumbel model best describe the marginal distribution of an annual maximum temperature and the corresponding low flow characteristics for station 2106.
4. The 2-parameter Logistic and 3-parameter GEV are identified as most justifiable in describing the marginal behaviour of the annual maximum temperature and the corresponding low flow series for station 2415.
5. Finally, at station 2473, 2-parameter Logistic and 2-parameter Lognormal distribution best describe the univariate marginal distribution of annual maximum temperature and the corresponding low flow characteristics.

From the above results, it is found that the 2-parameter Logistic model performed better for most of the stations. The validity of the above-selected 1-D models is examined further by performing some qualitative-based graphical visual inspection. For instance, comparative PDF plots, CDF plots, P-P (probability-probability) plots and Q-Q (quantiles-quantiles) plots of each fitted candidate model at each station (refer to Supplementary Figures (SF (4a-d), SF (5a-d), SF (6a-d), SF (8a-d), SF (9-a-d) SF (10a-d) SF (11a-d)). The visual inspection entirely agrees with the quantitative measuring approach. In conclusion, the above-selected best-fitted marginal distributions are introduced in the joint dependency modelling using the most parsimonious 2-D copula function selected for each station.

4.2. Strength of dependency measures

Before selecting an appropriate 2-D copula function, investigating the degree of mutual concurrency between selected historical extrema pairs is often a mandatory prerequisite. This study calculated both the parametric Pearson correlation coefficient (r) and the nonparametric rank-based Kendall's tau (τ) and Spearman's rho (ρ). The Pearson dependence measure is not invariant to monotonic transformation, which cannot capture nonlinear dependencies and is incompatible with heavy-tailed distribution (Tosunglou and Kisi 2016). Both the nonparametric dependence statistics have high resistance to an outlier. They are also invariant under the monotonic nonlinear transformation (Klein et al., 2011) and thus can result in much more effective dependence measures in a nonlinear framework. Table 2 lists the estimated dependence (or correlation coefficient) measures for each station where all the statistics are measured at the 5% significance level (95% confidence interval). It is found that a significant negative correlation is found at each station, and thus only the negative dependence copula model was selected in the bivariate joint simulation.

Insert Table 2

Some visual inspection is also carried out, for instance, via Chi plot (Fisher and Switzer 2001), Kendall plot (K-plot) (Genest and Boies 2003) and 2-D scatterplot (refer to Supplementary Figures (SF 12a-b to 16 a-b)). The Chi-plot is a scatterplot of the pairs $(\lambda_i \chi_i)$, uses the data ranks, and where $'\lambda_i'$ values measure the distance of bivariate observations from the centre of the data sets within a range of [-1, 1]. If a stronger dependency is exhibited, the random pairs must be outside control limit range of the Chi-plot. It is found that most of the random pairs are outside this control limit range for all the selected stations.

On the other hand, the deviation of random pairs from the main diagonal of the 2-D K-plot must indicate high (with significant) dependency; otherwise, when the plot is near to linear (or closer to 45° Angle), it must indicate independence (Reddy and Ganguli 2013). Most of the dataset, for all stations, is away on the right side of this linear line. Similarly, the 2-D scatterplots for each station indicate a higher dependency level (or negatively correlated variables). In conclusion, all three 2-D plots collectively show a significant negative correlation between random pairs for each station and support the quantitative approach of dependence measures. Each station's dependence measures statistics confirmed the possibility of a 2-D copula structure in modelling the joint correlation structure between maximum river temperature and corresponding low flow.

4.3. Joint dependence modelling between maximum temperature and low flow

The efficacy of eighteen different negatively dependent 2-D copula classes, were tested. The copula dependence parameters are estimated using MPL estimators, followed by Equation 6 (refer to section 2.2). The estimated copulas parameters are listed in Tables 3 (a-e).

Insert Tables 3 (a-e)

The Cramer-von Mises (CvM) distance statistics with a parametric bootstrapping procedure are adopted to analyze the performance of the most justifiable 2-D copulas from different candidate models in describing bivariate joint dependencies, followed by Equations 7 and 8 (refer to section 2.3). In this approach, the CvM functional statistics $'S_n'$ and its associated p-value are estimated using simulated random pairs (bootstrapping samples, N=1000) via a parametric bootstrapping approach. The best-fitted 2-D copula must have the minimum value of S_n statistics with an estimated (p-value > 0.05). It is found that the rotated Clayton copula (90 degrees) (fit best for station 2044), the rotated BB8 Copula (for station 2084), the rotated Joe Copula (90 degrees) (fit best for station 2106), the rotated Tawn type-1 Copula (90 degrees) (fit best for station 2415), and rotated Clayton Copula (90 degrees) (fit best for station 2473). Tables 3 (a-e) list the estimated GOF test statistics of each station's candidate copulas.

The performance of the selected bivariate copulas for each station is examined graphically using an overlapped scatterplot between historical bivariate random pairs with a set of generated pairs (sample size, N=1000) estimated from the best-fitted copulas (refer to Supplementary Figures (SF 17 a-h)). The selected 2-D copulas perform adequately since the generated random pairs (in light blue) overlapped with the natural mutual dependence of the historical samples (in red) for all selected stations.

Besides this, the suitability and reliability of the selected copulas selected for each station are investigated further by comparing Kendall's tau (τ) correlation statistics, estimated from the generated random samples (N = 1000) using the best-fitted 2-D Copula and compared with the empirical Kendall's tau (τ) coefficient estimated from the historical observations (refer to Supplementary Table ST7). All the selected 2-D copulas exhibit minimum gaps or differences between empirical and theoretical Kendall's tau (τ); in other words, these selected models can regenerate the mutual dependence of historical random pairs more effectively.

4.4. Joint and conditional probability distribution and their associated return periods

4.4.1. Estimation of primary joint return periods for river temperature and corresponding low flow

The best-fitted 2-D copulas are employed with best-fitted univariate marginal distributions (section 4.1) in bivariate joint cumulative distribution functions (JCDFs) and joint probability density functions (JPDFs) (refer to Supplementary Figures SF 19(a-d)-23(a-d)). The estimated JCDFs is employed further in estimating primary joint return periods for both OR- and AND-joint cases for the different scenario of bivariate annual maximum temperature and corresponding low flow, followed by Equations 9 and 10 (see section 2.4.2). Supplementary Figure 19 (a-d) (right side figure) illustrates the bivariate joint cumulative density contours.

The bivariate versus univariate return periods for a different combination of annual maximum water temperature and corresponding low flow series are listed in Tables 4 (a-e). The design variables quantiles of various return periods, for instance, 2, 5, 10, 20, 30, 50, 79, and 100 years for each station, are estimated in these tables' 4th and 5th columns using the inverse of the best-fitted univariate marginal CDFs (or quantiles function). Both the bivariate OR- and AND-joint returns are estimated for different designed or synthetic pairs of annual maximum river temperature and corresponding low flow (estimated at different annual exceedance probabilities (AEP)) in the 8th and 9th columns of Tables 4 (a-e). This table shows that the value of AND-joint return periods for any bivariate design events is higher than OR-joint return periods. In other words, the occurrence of bivariate events (i.e., annual maximum river temperature and corresponding low flow) simultaneously is less frequent in the AND-joint case as compared to the OR-joint event case for all stations, $\mathrm{T}^{\mathrm{OR}} < \mathrm{T}^{\mathrm{AND}}$.

When considering ecologically relevant temperature thresholds (e.g., 15℃ or between 13.1℃ to 13.9℃), from Tables 4 (a-e), it is confirmed that river water temperature quantiles with low return periods (e.g., 2 years or 10 years) are above this critical value for all selected stations. Supplementary Figures (SF 24 a-b) show the box plots of annual maximum river temperature and corresponding low flow measured at different return periods. For instance, at station 2044, the annual maximum river temperature is 25.05 ℃, and station 2106 is 21.70 ℃ when considering the return of 2 years. Similarly, at 10-year return periods, the river temperature quantile is 26.67 ℃ (at station 2044), 23.22 ℃ (at station 2106) etc. The growth of brown trout (*Salmo trutta*) can cease when the temperature rises above 18.7-19.5 ℃; also, it can influence vitellogenin (Vtg) concentration in brown trout's plasma when the temperature rises above 19℃. Table 4 (a-e) shows that all stations, except 2473, have river temperature quantiles above this threshold at low return periods (2 years or above). Station 2473 attained river temperature quantiles above this threshold at return periods 30 years or above, while station 2084 temperature quantiles exceeded this threshold when its return period is 5 years or above.

Besides this, corresponding low-flow quantiles are compared for different stations using the values of estimated absolute discharge and their specific discharge values at different return periods (refer to Table 4 a-e and SF24b, SF25 and SF26). For instance, at a 2-year return period, the low flow discharge value is 14.73 m^3/sec (at station 2044), 8.24 m^3/sec (at station 2084), 4.34 m^3/sec (at station 2106) etc. For the same stations, at the same return periods, the specific discharge values are 0.00862 $\frac{\mathrm{m}^3}{\mathrm{sec}}/\mathrm{km}^2$, 0.02618 $\frac{\mathrm{m}^3}{\mathrm{sec}}/\mathrm{km}^2$, 0.00460 $\frac{\mathrm{m}^3}{\mathrm{sec}}/\mathrm{km}^2$ etc. From the SF26 (box plot) and SF27 (line graph), it is illustrated that station 2084 has a higher specific discharge value than other stations observed at different return periods; it has a smaller drainage basin surface area (314.76 km^2). For instance, at a return period of 10 years, the estimated corresponding low flow is 21.75 m^3/sec at station 2084, which is lower than station 2473, which has an estimated low flow value of 252.16 m^3/sec. However, because of the larger basin surface area of station 2473 (6299.198 km^2), it exhibited a lower specific discharge value than station 2084. Conversely, the ratio of estimated low flow with its drainage surface area for station 2106 is minimum compared to other stations for different return periods.

When the joint return periods for both OR- and AND- cases are examined, the AND-joint case has higher return periods than univariate return periods for both water temperature and corresponding low flow. Supplementary Figures (SF28 (a-e)) illustrate the simulated or synthetic (N=10,00000) bivariate random pairs using the best-fitted copula joint distribution for each station. Most generated bivariate random pairs lie within the yellow square box. For instance, for station 2044, most simulated annual bivariate samples have maximum river temperature values lying between 20℃ to 30℃, and corresponding low flow values are below 40 m^3/s (and their absolute discharge values are below 0.02340 $\frac{m^3}{sec}/km^2$). However, for station 2473, the corresponding streamflow of most simulated sample values is above 80 m^3/s. Its specific discharge value is above 0.01270 $\frac{m^3}{sec}/km^2$, but most of its simulated river temperature sample values are between 15℃ to 23℃. For other stations, e.g., 2106 (absolute discharge is below 15 m^3/sec, and specific discharge is below 0.01591 $\frac{m^3}{sec}/km^2$ together with most river temperature samples ranging between 18℃ to 29℃), 2415 (discharge is below 15 m^3/sec, and specific discharge of most simulated samples are below 0.03589 $\frac{m^3}{sec}/km^2$ with river temperature samples are ranging between 20℃ to 30℃). For station 2084, most of its river temperature samples lie between 13℃ to 24℃, but its flow value is below 60 m^3/sec (and the specific discharge value is below 0.19062 $\frac{m^3}{sec}/km^2$). This bivariate estimated quantile reveals that river flow characteristics at station 2473 are relatively better than other selected stations. From Table 4 (a-e), it is already confirmed that station 2473 has a higher low flow value estimated at different return periods together with the largest drainage basin area compared to other stations. Also, for stations 2044, 2106, and 2415, some samples' upper river temperature reaches about 30℃. For station 2415, some samples' lower river temperature value is about 20℃.

Also, we are presenting a brief discussion of obtained bivariate return periods only for stations 2044 and 2415 because of limited space. Let us consider, at station 2044, a 10-year return period of extreme events having the following characteristics (refer to Table 4a), annual maximum water temperature = 26.67℃, and corresponding low series = 21.17 m^3/s, the bivariate return period for OR- and AND- joint case is, T^{OR} = 5.01 years and T^{AND} = 3234.15 years. Conversely, their univariate return period for this univariate design value is 10 years. Similarly, at 2-year return periods, the design variables, for instance, annual maximum temperature = 25.08℃, and corresponding low flow = 14.73 m^3/s, the bivariate joint return periods for OR-event is 1.16 years, and AND-event is 7.22 years. It is found that, for every station, OR-joint returns are less than the univariate return periods and AND-joint event case for any combination of the design variables. These estimated statistics reveal that considering only a univariate return period (for instance, via extreme water temperature) would be problematic; it can mislead the risk assessments when compounding the joint occurrence of both variables. It is also found that the OR-joint return period is nearly half the value of the univariate return periods.

By analyzing the co-occurrence probabilities or mutual risk of river water temperature and low flow using the AND-joint return case for all stations and applying Equations 9 & 10, it was discovered that station 2415 has the lowest AND return period values compared to other stations with the same AEP..E.For instance, for 10-year return periods (AEP = 0.10 or NEP=0.9), the bivariate AND-joint return is 130 years, which is less than other stations, e.g., T^{AND} = 6830.60 years (station 2106) > 3234.15 years (station 2044) > 1332.98 years (station 2473) > 1041.78 years (station 2084) (refer to Tables 4 (a-e)). Supplementary Figures (SF 29 (a-b)) illustrate the box plots of the estimated bivariate joint return periods for OR and AND-joint cases using observed historical events for each station. Likewise, the other station follows the same: bivariate AND-returns > Univariate returns > OR-returns.

In conclusion, all the above-estimated results and their detailed comparison confirmed that the compound effect of annual maximum temperature and corresponding low flow results in additional information for water resources and fish habitat management compared with univariate analyses.

Insert Table 4 (a-e)

4.4.2. Estimation of conditional joint return periods

Two different conditional joint relationships are considered in this study, $T_{A|B>b}$ (Equation 11) and $T_{A|B\leq b}$ (Equation 12) (refer to Figures 3 (a-d) to Figures 7 (a-d)).

Because of the word limit, we are presenting a brief discussion only for Station 2044 (Figure 3). For both conditional joint cases, the return period of bivariate events increases with an increase in the percentile values of the conditional variable, corresponding low flow (Figures 3a, b) or annual maximum temperature (Figures 3c, d). The conditional relationship estimated for the case, $T_{A|B>b}$ attained higher return periods than the case $T_{A|B\leq b}$, for all the selected stations. For instance, on July 18, 1976, have annual maximum temperature was 26.55℃, the conditional return period was 21.66 years (when corresponding low flow > 8.046 m^3/s (5th percentile)), 63.87 years (when low flow > 11.03 m^3/s (25th percentile)), and 451.25 years (when low flow > 14.91 m^3/s (50th percentile)), 2495.86 years (when corresponding low flow > 17.82 m^3/s (75th percentile)) and so on. On the other side, for conditional case $T_{A|B\leq b}$, for the same station and calendar date, the return period was 1.38 years (when low flow ≤ 8.046 m^3/s (5th percentile)), 2.25 (when low flow ≤ 11.03 m^3/s (25th percentile)), 4.55 (when low flow ≤ 14.91 m^3/s (50th percentile)), 6.37 (when low flow ≤ 17.82 m^3/s (75th percentile)) and so on.

Similarly, when considering the annual maximum water temperature as a conditioning variable, the conditional JRPs of low flow increase with an increase in the percentile value of the annual maximum temperature. For instance, on the same calendar date, July 18, 1976, having a corresponding low flow value is 8.06 m^3/s, the conditional joint return is 1.27 years and 1.002 years when the annual maximum temperature > 23.13℃ and ≤ 23.13℃ respectively (both at the 5th percentile), 1.86 years and 1.003 years when the annual maximum temperature > 24.15℃ and ≤ 24.15℃ respectively (both at the 25th percentile), and 187.84 years and 1.03 years respectively when the annual maximum temperature > 26.584℃ and ≤ 26.584℃ (both at the 90th percentile).

Besides this, for the same station 2044, by fixing the percentile values at, say, the 5th percentile (i.e., corresponding low flow > 8.046 m^3/s), the return period is 6.21 years (when the water temperature is 25.84℃, on July 25, 1969), 21.66 years (when the water temperature is 26.55℃, on July 18, 1976), 262.81 years (when the water temperature is 27.49℃, on July 31, 1983). Similarly, by fixing the percentile value at 5% percentile (i.e., annual maximum temperature > 23.15℃), the return period is 4.17 years (when the corresponding low flow is 17.30 m^3/s, on July 25, 1969), 1.27 years (when the corresponding low flow is 8.06 m^3/s, on July 18, 1976), the return period is 1.27 years (when the low flow is 8.02 m^3/s, on July 31, 1983) and so on.

In conclusion, the above discussion reveals the importance of considering the conditional joint distribution relationship between variable interest and a joint return period in the risk assessment of aquatic habitats and fish management.

5. Research Conclusions

Understanding the joint probability distribution of extreme river temperature and low flow is crucial for assessing risk in water resources and fish habitat management. Considering only one variable as a stress indicator may result in incomplete or underestimated risk assessments because both events are negatively correlated, and their joint impact could be harmful. To properly study the joint impact, multivariate joint probability analysis and the concept of multivariate exceedance probability are necessary. This study used a copula-based methodology to analyze the bivariate joint distribution of annual maximum river water temperature and corresponding low flow for five stations in Switzerland. The efficacy of seven parametric class 1-D probability distributions and eighteen negatively dependent parametric class 2-D copulas was tested and fitted via MLE and MPL estimation procedures. The most justifiable copula for each station and selected marginal distributions were used to estimate joint exceedance probabilities and their associated joint and conditional joint return periods. The results showed a significant negative correlation between water temperature and low flow at all stations. The bivariate return was higher in the AND-joint case than in the OR-joint case or univariate return periods, meaning that both events are less likely to co-occur than for just one of them to occur. It is essential to consider both joint return periods, as focusing solely on either the OR or AND joint case would be problematic.

According to the information gathered from SF (24a-e), most of the simulated bivariate random observation values for river temperature are above 18℃, while the corresponding low flow values for selected stations are below 50 m^3/s. This could potentially increase the risk of PKD disease in brown trout populations or affect the plasma concentration of vitellogenin (Vtg). Furthermore, the conditional joint return periods of river temperature given various percentile values of corresponding low flow and their vice-versa are also examined for two different conditional joint cases. It is found that the joint return periods of bivariate events with extreme river temperatures increase as the percentile value of low flow (conditioning variable) increases. Also, higher maximum river temperatures result in higher bivariate return periods than lower river temperatures at the same conditioning variable (low flow series). As the river water temperature increases (as a conditioning variable), the return periods of low flow for the bivariate event also increase. In conclusion, the above-discussed bivariate return periods and estimated quantiles help us gain valuable insights into the relative joint river thermal-low flow risk for water species in Swiss rivers.The present study has some limitations that will require further considerations in future studies:

1. Parametric class distribution often has limitations in the context of prior distributional assumptions. Incorporating the multivariate copula in the parametric settings requires distributional assumptions for their univariate marginals PDFs and copula joint density (e.g., Archimedean, Elliptical, etc.). It could be a risk of misspecification if the underlying statistical assumptions of the selected predefined marginals PDF and/or copula density are violated and can lack flexibility which is already pointed out in some previous studies such as Charpentier et al. (2006) and Rauf and Zeephongsekul (2014). On the other hand, many of the existing studies already pointed out that if data exhibited asymmetrical (or skewed) behaviour, the performance of the distribution-free-based nonparametric kernel density function would be better than a parametric formulation (Adamowski 2000; Kim et al., 2006). Kernel density is a data-driven nonparametric density function approximation approach, often revealing bonafide density functions (Dooge 1986; Santhosh and Srinivas 2014).

2. The present study found that variable annual maximum river temperatures for stations 2044 and 2084 are nonstationary. This study is not considering the impact of time-varying consequences due to dynamic environmental arising or climate change in modelling univariate marginal or multivariate copula dependence structure. The impact of climate change may alter river water temperature through a different mechanism, for instance, by reducing river water flow by increasing evaporation or fewer rainfall events. On the other side, there will directly impact the behaviour of streamflow (or low flow) due to changes in catchment characteristics due to large-scale human intervention. Also, the river water temperature can alter when there is an increased demand for water, for instance, irrigation. Milley et al. (2008) stated that considering stationary assumptions in the hydrological data series in multivariate frequency analysis may no longer be valid. It is crucial to consider eventual nonstationarities in the data to reflect their impacts on the estimated univariate or multivariate exceedance probabilities or return periods.

CRediT authorship contribution statement

Shahid L: Conceptualization, Methodology, Software, Formal analysis, Validation, Writing-original draft preparation, Project administration**. Souaissi Z:** Conceptualization, Methodology, Investigation, Validation, Writing-Original draft preparation, **Taha B.M.J Ouarda:** Project Focus and Supervision, Funding acquisition, Conceptualization, Methodology, Project administration, Writing-Review & editing, Results validations**, André- St-Hilaire:** Project focus, Conceptualization, Methodology, Writing-Review & editing, Results validations.

Declaration of Competing Interest

The authors declare that they have no known competing financial interests or personal relationships that could have appeared to influence the work reported in this manuscript.

Acknowledgements

The authors thank the National Sciences and Engineering Research Council of Canada (NSERC) and the Canada Research Chair Program for funding this research. Also, we would like to thank the Federal Office of the Environment (FOEN) of Switzerland (https://www.bafu.admin.ch/bafu/en/home/topics/water/state.html) for providing us with daily-basis river water temperature and low flow data for Switzerland. The authors would like to extend their gratitude to Prof. Xuebin Zhang, the Editor-in-Chief, and two anonymous reviewers for their comments and suggestions, which significantly enhanced the quality of the paper.

6. References

Abidi, O., St-Hilaire, A., Ouarda, T. B. M. J., Charron, C., Boyer, C., & Daigle, A. (2022). Regional thermal analysis approach: A management tool for predicting water temperature metrics relevant for thermal fish habitat. Ecological Informatics, 70, 101692. https://doi.org/10.1016/j.ecoinf.2022.101692.

Adamowski, K. (1985). Nonparametric Kernel Estimation of Flood Frequencies. Water Resources Research, 21(11), 1585–1590. Portico. https://doi.org/10.1029/wr021i011p01585.

Adamowski, K. (2000). Regional analysis of annual maximum and partial duration flood data by nonparametric and L-moment methods. Journal of Hydrology, 229(3–4), 219–231. https://doi.org/10.1016/s0022-1694(00)00156-6.

AghaKouchak, A., Sellars, S., & Sorooshian, S. (2012). Methods of Tail Dependence Estimation. Water Science and Technology Library, 163–179. https://doi.org/10.1007/978-94-007-4479-0_6.

Alobaidi, M. H., Ouarda, T. B. M. J., Marpu, P. R., & Chebana, F. (2021). Diversity-driven ANN-based ensemble framework for seasonal low-flow analysis at ungauged sites. Advances in Water Resources, 147, 103814. https://doi.org/10.1016/j.advwatres.2020.103814.

Alam, A., Bhat, M. S., Farooq, H., Ahmad, B., Ahmad, S., & Sheikh, A. H. (2018). Flood risk assessment of Srinagar city in Jammu and Kashmir, India. International Journal of Disaster Resilience in the Built Environment, 9(2), 114–129. https://doi.org/10.1108/ijdrbe-02-2017-0012.A

lina B (2018). Copula Modeling for world's biggest competitors. Master Thesis, Amsterdam School of Economics, University of Amsterdam.

Anderson, T. W., & Darling, D. A. (1954). A Test of Goodness of Fit. Journal of the American Statistical Association, 49(268), 765–769. https://doi.org/10.1080/01621459.1954.10501232.Boyer, C., St-Hilaire, A., & Bergeron, N. E. (2021). Defining river thermal sensitivity as a function of climate. River Research and Applications, 37(10), 1548–1561. Portico. https://doi.org/10.1002/rra.3862.Bobée, B., & Ashkar, F. (1989). Log-logistic flood frequency analysis — Comment. Journal of Hydrology, 107(1–4), 367–370. https://doi.org/10.1016/0022-1694(89)90067-x.

Breau, C., Cunjak, R. A., & Bremset, G. (2007). Age-specific aggregation of wild juvenile Atlantic salmon Salmo salar at cool water sources during high temperature events. Journal of Fish Biology, 71(4), 1179–1191. https://doi.org/10.1111/j.1095-8649.2007.01591.x.

Booker, D. J., & Whitehead, A. L. (2021). River water temperatures are higher during lower flows after accounting for meteorological variability. River Research and Applications, 38(1), 3–22. Portico. https://doi.org/10.1002/rra.3870.

Bras RL (1990). Hydrology: an introduction to hydrologic science. Addison-Wesley ISBN 0201059223:9780201059229.Buishand, T. A. (1982). Some methods for testing the homogeneity of rainfall records. Journal of Hydrology, 58(1–2), 11–27. https://doi.org/10.1016/0022-1694(82)90066-x.

Caissie, D., Ashkar, F., & El-Jabi, N. (2019). Analysis of air/river maximum daily temperature characteristics using the peaks over threshold approach. Ecohydrology, 13(1). Portico. https://doi.org/10.1002/eco.2176.CAISSIE, D. (2006). The thermal regime of rivers: a review. Freshwater Biology, 51(8), 1389–1406. https://doi.org/10.1111/j.1365-2427.2006.01597.x.

Caissie, D., Satish, M. G., & El-Jabi, N. (2007). Predicting water temperatures using a deterministic model: Application on Miramichi River catchments (New Brunswick, Canada). Journal of Hydrology, 336(3–4), 303–315. https://doi.org/10.1016/j.jhydrol.2007.01.008.

Charron, C., & Ouarda, T. B. M. J. (2015). Regional low-flow frequency analysis with a recession parameter from a nonlinear reservoir model. Journal of Hydrology, 524, 468–475. https://doi.org/10.1016/j.jhydrol.2015.03.005.

Chebana, F., & Ouarda, T. B. M. J. (2021). Multivariate nonstationary hydrological frequency analysis. Journal of Hydrology, 593, 125907. https://doi.org/10.1016/j.jhydrol.2020.125907.

Chebana, F., & Ouarda, T. B. M. J. (2009). Index flood-based multivariate regional frequency analysis. Water Resources Research, 45(10). Portico. https://doi.org/10.1029/2008wr007490.

Constantino, M., Larran, M., & Brebbia, C.A. (2008). Computational finance and its applications III, Volume 41 of W.I.T. transactions on information and communication technologies, W.I.T. Press, 2008. https://doi.org/10.2495/cf08.

Cramér, H. (1928). On the composition of elementary errors. Scandinavian Actuarial Journal, 1928(1), 13–74. https://doi.org/10.1080/03461238.1928.10416862.

Daigle, A., St-Hilaire, A., Beveridge, D., Caissie, D., & Benyahya, L. (2011). Multivariate analysis of the low-flow regimes in eastern Canadian rivers. Hydrological Sciences Journal, 56(1), 51–67. https://doi.org/10.1080/02626667.2010.535002.

De Michele, C. (2003). A Generalized Pareto intensity-duration model of storm rainfall exploiting 2-Copulas. Journal of Geophysical Research, 108(D2). https://doi.org/10.1029/2002jd002534.

De Michele, C., Salvadori, G., Vezzoli, R., & Pecora, S. (2013). Multivariate assessment of droughts: Frequency analysis and dynamic return period. Water Resources Research, 49(10), 6985–6994. Portico. https://doi.org/10.1002/wrcr.20551.

D.F.O., (2013). Framework for Assessing the Ecological Flow Requirements to Support Fisheries in Canada. D.F.O. Can. Sci. Advis. Rep. 2013/017.

Durrans, S. R., Ouarda, T. B. M. J., Rasmussen, P. F., & Bobée, B. (1999). Treatment of Zeroes in Tail Modeling of Low Flows. Journal of Hydrologic Engineering, 4(1), 19–27. https://doi.org/10.1061/(asce)1084-0699(1999)4:1(19).

Elliott, & Hurley. (2001). Modelling growth of brown trout, Salmo trutta, in terms of weight and energy units. Freshwater Biology, 46(5), 679–692. Portico. https://doi.org/10.1046/j.1365-2427.2001.00705.x.

Elliott, J. M., & Elliott, J. A. (2010). Temperature requirements of Atlantic salmon Salmo salar, brown trout Salmo trutta and Arctic charr Salvelinus alpinus: predicting the effects of climate change. Journal of Fish Biology, 77(8), 1793–1817. https://doi.org/10.1111/j.1095-8649.2010.02762.x.

El Adlouni, S., Ouarda, T. B. M. J., Zhang, X., Roy, R., & Bobée, B. (2007). Generalized maximum likelihood estimators for the nonstationary generalized extreme value model. Water Resources Research, 43(3). Portico. https://doi.org/10.1029/2005wr004545.

Environment Agency. (2008). The thermal biology of brown trout and Atlantic salmon. https://assets.publishing.service.gov.uk/government/uploads/system/uploads/attachment_data/file/291742/scho1008boue-e-e.pdf. [Extraction date: 2023-02-08].

Escalante-Sanboval, C. A., & Raynal-Villasenor, J. A. (1998). Multivariate estimation of floods: the trivariate gumbel distribution. Journal of Statistical Computation and Simulation, 61(4), 313–340. https://doi.org/10.1080/00949659808811917.

Fan, Y. R., Huang, W. W., Huang, G. H., Huang, K., Li, Y. P., & Kong, X. M. (2015). Bivariate hydrologic risk analysis based on a coupled entropy-copula method for the Xiangxi River in the Three Gorges Reservoir area, China. Theoretical and Applied Climatology, 125(1–2), 381–397. https://doi.org/10.1007/s00704-015-1505-z.

Farrell, P. J., & Rogers-Stewart, K. (2006). Comprehensive study of tests for normality and symmetry: extending the Spiegelhalter test. Journal of Statistical Computation and Simulation, 76(9), 803–816. https://doi.org/10.1080/10629360500109023.

Ficklin, D. L., Stewart, I. T., & Maurer, E. P. (2013). Effects of climate change on stream temperature, dissolved oxygen, and sediment concentration in the Sierra Nevada in California. Water Resources Research, 49(5), 2765–2782. Portico. https://doi.org/10.1002/wrcr.20248.

Fullerton, A. H., Burnett, K. M., Steel, E. A., Flitcroft, R. L., Pess, G. R., Feist, B. E., Torgersen, C. E., Miller D. J., & Sanderson, B. L. (2010). Hydrological connectivity for riverine fish: measurement challenges and research opportunities. Freshwater Biology, 55(11), 2215–2237. Portico. https://doi.org/10.1111/j.1365-2427.2010.02448.x.

Fisher, N. I., & Switzer, P. (2001). Graphical Assessment of Dependence. The American Statistician, 55(3), 233–239. https://doi.org/10.1198/000313001317098248.

Ganguli, P., & Reddy, M. J. (2012). Risk Assessment of Droughts in Gujarat Using Bivariate Copulas. Water Resources Management, 26(11), 3301–3327. https://doi.org/10.1007/s11269-012-0073-6.

Genest, C., & Boies, J.-C. (2003). Detecting Dependence With Kendall Plots. The American Statistician, 57(4), 275–284. https://doi.org/10.1198/0003130032431.

Genest, C., & Rémillard, B. (2008). Validity of the parametric bootstrap for goodness-of-fit testing in semiparametric models. Annales de l'Institut Henri Poincaré, Probabilités et Statistiques, 44(6). https://doi.org/10.1214/07-aihp148.

Genest, C., & Rivest, L.-P. (1993). Statistical Inference Procedures for Bivariate Archimedean Copulas. Journal of the American Statistical Association, 88(423), 1034–1043. https://doi.org/10.1080/01621459.1993.10476372.

Genest, C., Ghoudi, K., & Rivest, L.-P. (1995). A semiparametric estimation procedure of dependence parameters in multivariate families of distributions. Biometrika, 82(3), 543–552. https://doi.org/10.1093/biomet/82.3.543.

Goel, N. K., Seth, S. M., & Chandra, S. (1998). Multivariate Modeling of Flood Flows. Journal of Hydraulic Engineering, 124(2), 146–155. https://doi.org/10.1061/(asce)0733-9429(1998)124:2(146).

Gringorten, I. I. (1963). A plotting rule for extreme probability paper. Journal of Geophysical Research, 68(3), 813–814. https://doi.org/10.1029/jz068i003p00813.

Grimaldi, S., & Serinaldi, F. (2006). Asymmetric copula in multivariate flood frequency analysis. Advances in Water Resources, 29(8), 1155–1167. https://doi.org/10.1016/j.advwatres.2005.09.005.

Gräler, B., van den Berg, M. J., Vandenberghe, S., Petroselli, A., Grimaldi, S., De Baets, B., & Verhoest, N. E. C. (2013). Multivariate return periods in hydrology: a critical and practical review focusing on synthetic design hydrograph estimation. Hydrology and Earth System Sciences, 17(4), 1281–1296. https://doi.org/10.5194/hess-17-1281-2013.

Hamza A., Ouarda, T.B.M.J., Durrans, R.S. & Bobée, B. (2001). Development of scaling and tail models for the regional estimation of low-flows, Canadian Journal of Civil Engineering; 28(2), 291-304. https://doi.org/10.1139/l00-121.

Hannah, D., Webb, BW., & Nobilis, F. (2008). Preface - River and stream temperature: dynamics, processes, models and implications. Hydrological Processes: 22, 889-901. https://doi.org/10.1002/hyp.6997.

Hosking, J. R. M., Wallis, J. R., & Wood, E. F. (1985). Estimation of the Generalized Extreme-Value Distribution by the Method of Probability-Weighted Moments. Technometrics, 27(3), 251–261. https://doi.org/10.1080/00401706.1985.10488049.

Hodgson, S., & Quinn, T. P. (2002). The timing of adult sockeye salmon migration into fresh water: adaptations by populations to prevailing thermal regimes. Canadian Journal of Zoology, 80(3), 542–555. https://doi.org/10.1139/z02-030.

Humphries, P., & Baldwin, D. S. (2003). Drought and aquatic ecosystems: an introduction. Freshwater Biology, 48(7), 1141–1146. Portico. https://doi.org/10.1046/j.1365-2427.2003.01092.x.

'International Association of Hydrological and Sciences (I.A.H.S.). https://iahs.info/.Johnson N.L. (1994) Continuous univariate distribution, Wiley New York, Vol 1.

Joshi, D., St-Hilaire, A., Ouarda, T. B. M. J., Daigle, A., & Thiemonge, N. (2016). Comparison of direct statistical and indirect statistical-deterministic frameworks in downscaling river low-flow indices. Hydrological Sciences Journal, 61(11), 1996–2010. https://doi.org/10.1080/02626667.2014.966719.

Joe, H. (1997). Multivariate models and multivariate dependence concepts. CRC press.

Joe, H., & Hu, T. (1996). Multivariate Distributions from Mixtures of Max-Infinitely Divisible Distributions. Journal of Multivariate Analysis, 57(2), 240–265. https://doi.org/10.1006/jmva.1996.0032.

Kao, S.-C., & Govindaraju, R. S. (2010). A copula-based joint deficit index for droughts. Journal of Hydrology, 380(1–2), 121–134. https://doi.org/10.1016/j.jhydrol.2009.10.029.

Khaliq, M. N., Ouarda, T. B. M. J., Ondo, J.-C., Gachon, P., & Bobée, B. (2006). Frequency analysis of a sequence of dependent and/or nonstationary hydro-meteorological observations: A review. Journal of Hydrology, 329(3–4), 534–552. https://doi.org/10.1016/j.jhydrol.2006.03.004.

Klein, B., Schumann, A. H., & Pahlow, M. (2010). Copulas – New Risk Assessment Methodology for Dam Safety. Flood Risk Assessment and Management, 149–185. https://doi.org/10.1007/978-90-481-9917-4_8.

Klein, B., Pahlow, M., Hundecha, Y., & Schumann, A. (2010). Probability Analysis of Hydrological Loads for the Design of Flood Control Systems Using Copulas. Journal of Hydrologic Engineering, 15(5), 360–369. https://doi.org/10.1061/(asce)he.1943-5584.0000204.

Kojadinovic, I., & Yan, J. (2010). Modeling Multivariate Distributions with Continuous Margins Using thecopulaRPackage. Journal of Statistical Software, 34(9). https://doi.org/10.18637/jss.v034.i09.

Körner, O., Kohno, S., Schönenberger, R., Suter, M. J.-F., Knauer, K., Guillette, L. J., & Burkhardt-Holm, P. (2008). Water temperature and concomitant waterborne ethinylestradiol exposure affects the vitellogenin expression in juvenile brown trout (Salmo trutta). Aquatic Toxicology, 90(3), 188–196. https://doi.org/10.1016/j.aquatox.2008.08.012.

Latif, S., & Mustafa, F. (2020). Parametric Vine Copula Construction for Flood Analysis for Kelantan River Basin in Malaysia. Civil Engineering Journal, 6(8), 1470–1491. https://doi.org/10.28991/cej-2020-03091561.

Latif, S., & Mustafa, F. (2021). Bivariate joint distribution analysis of the flood characteristics under semiparametric copula distribution framework for the Kelantan River basin in Malaysia. Journal of Ocean Engineering and Science, 6(2), 128–145. https://doi.org/10.1016/j.joes.2020.06.003.

Latif, S., & Simonovic, S. P. (2022a). Parametric Vine Copula Framework in the Trivariate Probability Analysis of Compound Flooding Events. Water, 14(14), 2214. https://doi.org/10.3390/w14142214.

Latif, S., & Simonovic, S. P. (2022b). Nonparametric Approach to Copula Estimation in Compounding The Joint Impact of Storm Surge and Rainfall Events in Coastal Flood Analysis. Water Resources Management, 36(14), 5599–5632. https://doi.org/10.1007/s11269-022-03321-y.

Latif, S., & Simonovic, S. P. (2022c). Trivariate Joint Distribution Modelling of Compound Events Using the Nonparametric D-Vine Copula Developed Based on a Bernstein and Beta Kernel Copula Density Framework. Hydrology, 9(12), 221. https://doi.org/10.3390/hydrology9120221.

Lee, T., Ouarda, T. B. M. J., & Yoon, S. (2017). KNN-based local linear regression for the analysis and simulation of low flow extremes under climatic influence. Climate Dynamics, 49(9–10), 3493–3511. https://doi.org/10.1007/s00382-017-3525-0.

Lee, T., Modarres, R., & Ouarda, T. B. M. J. (2012). Data-based analysis of bivariate copula tail dependence for drought duration and severity. Hydrological Processes, 27(10), 1454–1463. https://doi.org/10.1002/hyp.9233.

Lima, C. H. R., Lall, U., Troy, T. J., & Devineni, N. (2015). A climate informed model for nonstationary flood risk prediction: Application to Negro River at Manaus, Amazonia. Journal of Hydrology, 522, 594–602. https://doi.org/10.1016/j.jhydrol.2015.01.009.

Li, F. (2016). Modeling covariate-contingent correlation and tail-dependence with copulas. https://arxiv.org/pdf/1401.0100.pdf.

López, J., & Francés, F. (2013). Nonstationary flood frequency analysis in continental Spanish rivers, using climate and reservoir indices as external covariates. Hydrology and Earth System Sciences, 17(8), 3189–3203. https://doi.org/10.5194/hess-17-3189-2013.

Lund, S. G., Caissie, D., Cunjak, R. A., Vijayan, M. M., & Tufts, B. L. (2002). The effects of environmental heat stress on heat-shock mRNA and protein expression in Miramichi Atlantic salmon (Salmo salar) parr. Canadian Journal of Fisheries and Aquatic Sciences, 59(9), 1553–1562. https://doi.org/10.1139/f02-117.

Manner, H. (2010). Modelling assymetric and time-varying dependence. https://cris.maastrichtuniversity.nl/portal/files/667227/guid-ae8195ad-cf0b%20-4744-8bb1-6a44fbe10fe7-ASSET1.0. [Accessed May 15, 2022].

McNeil, J., R. Frey, & Embrechts, P. (2005) Quantitative Risk Management: Concepts, Techniques and Tools, Princeton University Press, Princeton, NJ, U.S.A., 2005.

McNeil, A.J., Frey, R., & Embrechts, P. (2015). Quantitative risk management. Princeton University Press, Princeton. ISBN: 978-0-691-03407-16627-8.

Michel, A., Brauchli, T., Lehning, M., Schaefli, B., & Huwald, H. (2020). Stream temperature and discharge evolution in Switzerland over the last 50 years: annual and seasonal behaviour. Hydrology and Earth System Sciences, 24(1), 115–142. https://doi.org/10.5194/hess-24-115-2020.

Nelsen RB (2006) An introduction to copulas. Springer, New York.

Nikoloulopoulos, A. K., Joe, H., & Li, H. (2012). Vine copulas with asymmetric tail dependence and applications to financial return data. Computational Statistics & Data Analysis, 56(11), 3659–3673. https://doi.org/10.1016/j.csda.2010.07.016.

Novak, Rachael, Kennen, J.G., Abele, R.W., Baschon, C.F., Carlisle, D.M., Dlugolecki, Laura, Eignor, D.M., Flotemersch, J.E., Ford, Peter, Fowler, Jamie, Galer, Rose, Gordon, L.P., Hansen, S.E., Herbold, Bruce, Johnson, T.E., Johnston, J.M., Konrad, C.P., Leamond, Beth, and Seelbach, P.W, 2016, Final EPA-USGS Technical Report:Protecting Aquatic Life from Effects of Hydrologic Alteration: U.S. Geological Survey Scientific Investigations Report 2016–5164, U.S. Environmental Protection Agency E.P.A. Report 822-R-156-007, 156 p., Final EPA-USGS Technical Report: Protecting Aquatic Life from Effects of Hydrologic Alteration.

Ouarda, T. B. M. J., Charron, C., & St-Hilaire, A. (2022). Regional estimation of river water temperature at ungauged locations. Journal of Hydrology X, 17, 100133. https://doi.org/10.1016/j.hydroa.2022.100133.

Ouarda, T. B. M. J., Haché, M., Bruneau, P., & Bobée, B. (2000). Regional Flood Peak and Volume Estimation in Northern Canadian Basin. Journal of Cold Regions Engineering, 14(4), 176–191. https://doi.org/10.1061/(asce)0887-381x(2000)14:4(176)

Ouarda, T. B. M. J., Charron, C., Hundecha, Y., St-Hilaire, A., & Chebana, F. (2018). Introduction of the G.A.M. model for regional low-flow frequency analysis at ungauged basins and comparison with commonly used approaches. Environmental Modelling & Software, 109, 256–271. https://doi.org/10.1016/j.envsoft.2018.08.031.

Ouarda, T. B. M. J., Charron, C., & St-Hilaire, A. (2008). Statistical Models and the Estimation of Low Flows. Canadian Water Resources Journal, 33(2), 195–206. https://doi.org/10.4296/cwrj3302195.

Owen, C.E.B. (2008) Parameter estimation for the beta distribution. All Thesis and Disertation, p 1614. https://scholarsarchive.byu.edu/etd/1614.

Pettitt, A. N. (1979). A Nonparametric Approach to the Change-Point Problem. Applied Statistics, 28(2), 126. https://doi.org/10.2307/2346729.

Petts, G. E. (2000). A perspective on the abiotic processes sustaining the ecological integrity of running waters. Assessing the Ecological Integrity of Running Waters, 15–27. https://doi.org/10.1007/978-94-011-4164-2_2.

R Core Team (2021). R: A language and environment for statistical computing. R Foundation for Statistical Computing, Vienna, Austria. URL https://www.R-project.org/.

Reddy, M. J. & Ganguli, P. (2011). Application of copulas for derivation of drought severity-duration-frequency curves. Hydrological Processes, 26(11), 1672–1685. https://doi.org/10.1002/hyp.8287.

Salvadori, G., Michele, C. D., Kottegoda, N. T., & Rosso, R. (2007). Extremes in Nature. Water Science and Technology Library. https://doi.org/10.1007/1-4020-4415-1

Salvadori G, De Michele C, Kottegoda NT & Rosso R (2007) Extremes in nature: an approach using copulas. Springer Science & Business Media.

Salvadori, G., & De Michele, C. (2006). Statistical characterization of temporal structure of storms. Advances in Water Resources, 29(6), 827–842. https://doi.org/10.1016/j.advwatres.2005.07.013.

Salvadori, G., & De Michele, C. (2004). Frequency analysis via copulas: Theoretical aspects and applications to hydrological events. Water Resources Research, 40(12). Portico. https://doi.org/10.1029/2004wr003133.

Salvadori, G. (2004). Bivariate return periods via 2-Copulas. Statistical Methodology, 1(1–2), 129–144. https://doi.org/10.1016/j.stamet.2004.07.002.

Sand-Jensen K., Pedersen, O., Binzer, T, & Borum, J, (2005), Contrasting Oxygen Dynamics in the Freshwater Isoetid Lobelia dortmanna and the Marine Seagrass Zostera marina. Annals of Botany, 96(4), 613–623. https ://doi.org/10.1093/aob/mci214.

Sandoval, C. E., & Raynal-Villasenor, J. (2008). Trivariate generalized extreme value distribution in flood frequency analysis. Hydrological Sciences Journal, 53(3), 550–567. https://doi.org/10.1623/hysj.53.3.550.

Salvadori, G., & De Michele, C. (2010). Multivariate multiparameter extreme value models and return periods: A copula approach. Water Resources Research, 46(10). Portico. https://doi.org/10.1029/2009wr009040

Santhosh, D., & Srinivas, V. V. (2013). Bivariate frequency analysis of floods using a diffusion based kernel density estimator. Water Resources Research, 49(12), 8328–8343. Portico. https://doi.org/10.1002/2011wr010777.

Saklar A (1959) Functions de repartition n dimensions et leurs marges. Publ Inst Stat Univ Paris 8:229–231.

Serinaldi, F. (2014). Dismissing return periods! Stochastic Environmental Research and Risk Assessment, 29(4), 1179–1189. https://doi.org/10.1007/s00477-014-0916-1.

Seo, J., Won, J., Choi, J., Lee, J., & Kim, S. (2022). A copula model to identify the risk of river water temperature stress for meteorological drought. Journal of Environmental Management, 311, 114861. https://doi.org/10.1016/j.jenvman.2022.114861.

Shiau, J. T. (2006). Fitting Drought Duration and Severity with Two-Dimensional Copulas. Water Resources Management, 20(5), 795–815. https://doi.org/10.1007/s11269-005-9008-9.

Sinokrot, B. A., & Gulliver, J. S. (2000). In-stream flow impact on river water temperatures. Journal of Hydraulic Research, 38(5), 339–349. https://doi.org/10.1080/00221680009498315.

Souaissi, Z., Ouarda, T. B. M. J., & St-Hilaire, A. (2021). River water temperature quantiles as thermal stress indicators: Case study in Switzerland. Ecological Indicators, 131, 108234. https://doi.org/10.1016/j.ecolind.2021.108234.

Souaissi, Z., Ouarda, T. B. M. J., St-Hilaire, A., & Ouali, D. (2023). Regional frequency analysis of stream temperature at ungauged sites using non-linear canonical correlation analysis and generalized additive models. Environmental Modelling & Software, 163, 105682. https://doi.org/10.1016/j.envsoft.2023.105682.

St-Hilaire, A., Caissie, D., Bergeron, N. E., Ouarda, T. B. M. J., & Boyer, C. (2021). Climate change and extreme river temperature. Climate Change and Extreme Events, 25–37. https://doi.org/10.1016/b978-0-12-822700-8.00011-1

Sraj, M., Bezak, N., & Brilly, M. (2014). Bivariate flood frequency analysis using the copula function: a case study of the Litija station on the Sava River. Hydrological Processes, 29(2), 225–238. https://doi.org/10.1002/hyp.10145.

Strepparava, N., Segner, H., Ros, A., Hartikainen, H., Schmidt-Posthaus, H., & Wahli, T. (2017). Temperature-related parasite infection dynamics: the case of proliferative kidney disease of brown trout. Parasitology, 145(3), 281–291. https://doi.org/10.1017/s0031182017001482.

St-Hilaire, A., Ouarda, T. B. M. J., Bargaoui, Z., Daigle, A., & Bilodeau, L. (2011). Daily river water temperature forecast model with a k-nearest neighbour approach. Hydrological Processes, 26(9), 1302–1310. https://doi.org/10.1002/hyp.8216.

Sundt-Hansen, L. E., Hedger, R. D., Ugedal, O., Diserud, O. H., Finstad, A. G., Sauterleute, J. F., Tøfte, L., Alfredsen, K., & Forseth, T. (2018). Modelling climate change effects on Atlantic salmon: Implications for mitigation in regulated rivers. Science of The Total Environment, 631–632, 1005–1017. https://doi.org/10.1016/j.scitotenv.2018.03.058.

Tang, Y., Huynh., V.N & Lawry, J (2015) Integrated uncertainty in knowledge modelling and decision making- 4th International Symposium, Proceedings, LNAI 9376, Springer-Verlag, 2015.

Tawn, J. A. (1988). Bivariate extreme value theory: Models and estimation. Biometrika, 75(3), 397–415. https://doi.org/10.1093/biomet/75.3.397.

Tonkin, Z., Stuart, I., Kitchingman, A., Thiem, J. D., Zampatti, B., Hackett, G., Koster, W., Koehn, J., Morrongiello, J., Mallen-Cooper, M., & Lyon, J. (2019). Hydrology and water temperature influence recruitment dynamics of the threatened silver perch Bidyanus bidyanus in a regulated lowland river. Marine and Freshwater Research, 70(9), 1333. https://doi.org/10.1071/mf18299.

Tosunoglu, F., & Kisi, O. (2016). Joint modelling of annual maximum drought severity and corresponding duration. Journal of Hydrology, 543, 406–422. https://doi.org/10.1016/j.jhydrol.2016.10.018.

Villarini, G., Smith, J. A., & Napolitano, F. (2010). Nonstationary modeling of a long record of rainfall and temperature over Rome. Advances in Water Resources, 33(10), 1256–1267. https://doi.org/10.1016/j.advwatres.2010.03.013.

von Mises, R. (1928). Wahrscheinlichkeit Statistik und Wahrheit. https://doi.org/10.1007/978-3-662-36230-3.

Wanders, N., Vliet, M. T. H., Wada, Y., Bierkens, M. F. P., & Beek, L. P. H. (Rens). (2019). High-Resolution Global Water Temperature Modeling. Water Resources Research, 55(4), 2760–2778. Portico. https://doi.org/10.1029/2018wr023250.

Xu, Y., Huang, G., & Fan, Y. (2015). Multivariate flood risk analysis for Wei River. Stochastic Environmental Research and Risk Assessment, 31(1), 225–242. https://doi.org/10.1007/s00477-015-1196-0.

Yue, S., & Wang, C. Y. (2004). A comparison of two bivariate extreme value distributions. Stochastic Environmental Research and Risk Assessment (SERRA), 18(2), 61–66. https://doi.org/10.1007/s00477-003-0124-x.

Yue, S. (1999). Applying Bivariate Normal Distribution to Flood Frequency Analysis. Water International, 24(3), 248–254. https://doi.org/10.1080/02508069908692168.

Yue, S. (2001). A bivariate gamma distribution for use in multivariate flood frequency analysis. Hydrological Processes, 15(6), 1033–1045. https://doi.org/10.1002/hyp.259.

Yue, S. (2000). The Gumbel logistic model for representing a multivariate storm event. Advances in Water Resources, 24(2), 179–185. https://doi.org/10.1016/s0309-1708(00)00039-7

Yue, S., Ouarda, T.B.M.J., Bobée, B., Legendre, P., & Bruneau, P. (1999). The Gumbel mixed model for flood frequency analysis. Journal of Hydrology, 226: 88-100.

Yue, S., Ouarda, T. B. M. J., & Bobée, B. (2001). A review of bivariate gamma distributions for hydrological application. Journal of Hydrology, 246(1–4), 1–18. https://doi.org/10.1016/s0022-1694(01)00374-2.

Zhang, L., & Singh, V. P. (2006). Bivariate Flood Frequency Analysis Using the Copula Method. Journal of Hydrologic Engineering, 11(2), 150–164. https://doi.org/10.1061/(asce)1084-0699(2006)11:2(150).

Zhang, R., Chen, X., Cheng, Q., Zhang, Z., & Shi, P. (2016). Joint probability of precipitation and reservoir storage for drought estimation in the headwater basin of the Huaihe River, China. Stochastic Environmental Research and Risk Assessment, 30(6), 1641–1657. https://doi.org/10.1007/s00477-016-1249-z.

List of Tables

Table 1. Mathematical description and associated statistical properties of the 2-D copula model

Copula function	Bivariate Copula $C_\theta(u,v)$	Parameter range (θ)	Generating function (or generator) $\phi(t)$
Clayton	$\left[\max\{u^{-\theta}+v^{-\theta}-1;0\}\right]^{-1/\theta}$	$0 \le \theta < \infty$	$\frac{1}{\theta}\left(t^{-\theta}-1\right)$
Frank	$\frac{-1}{\theta}\ln\left(1+\frac{\left(e^{-\theta u}-1\right)\left(e^{-\theta v}-1\right)}{\left(e^{-\theta}-1\right)}\right)$	$-\infty < \theta < \infty$	$-\ln\left(\frac{e^{-\theta t}-1}{e^{-\theta}-1}\right)$
Gumbel-Hougaard (GH)	$\exp\left\{-\left[(-\ln(u))^{\theta}+(-\ln(v))^{\theta}\right]^{\frac{1}{\theta}}\right\}$	$1 \le \theta < \infty$	$(-\ln t)^{\theta}$
Joe	$1-\left[(1-u)^{\theta}+(1-v)^{\theta}-(1-u)^{\theta}(1-v)^{\theta}\right]^{1/\theta}$	$1 \le \theta < \infty$	$-\ln\left(1-(1-t)^{\theta}\right)$
BB1	$\left(1+\left[\left(u^{-\theta}-1\right)^{\delta}+\left(v^{-\theta}-1\right)^{\delta}\right]^{1/\delta}\right)^{-1/\theta}$	$0 < \theta < \infty$; $1 \le \delta < \infty$	
BB6	$1-\left(1-\exp-\left[\left(\left(-\ln(1-u)^{\theta}\right)\right)^{\delta}+\left(\left(-\ln\left(1-(1-v)^{\theta}\right)\right)^{\delta}\right)\right]^{1/\delta}\right)^{1/\theta}$	$1 \le \theta < \infty$; $1 \le \delta < \infty$	
BB7	$1-\left[1-\left(\left(1-u^{\theta}\right)^{-\delta}+\left(1-v^{\theta}\right)^{-\delta}-1\right)^{-1/\delta}\right]^{1/\theta}$	$1 \le \theta < \infty$; $0 \le \delta < \infty$	$\left(1-(1-t)^{\theta}\right)^{-\delta}-1$
BB8	$\frac{1}{\theta}\left(1-\left[1-\frac{1}{1-(1-\delta)^{\theta}}(1-(1-\delta u)^{\theta}(1-\delta v)^{\theta})\right]^{\frac{1}{\delta}}\right)$	$1 \le \theta < \infty$; $0 \le \delta \le 1$	$-\ln\left[\frac{1-(1-\delta t)^{\theta}}{1-(1-\delta)^{\theta}}\right]$

Note: θ is the copula dependence parameter of monoparametric copulas; θ and δ are the copula dependence parameters for bi-parametric (or 2-parameter) Archimedean copulas such as BB1, BB6, BB7 & BB8. This study employs the rotated version of the above copulas by 90 and 270 degrees, for instance, the rotated version of Clayton Joe, Gumbel by 90 degrees, the rotated version of BB1, BB6, BB7, and BB8 by 90 and 270 degrees.

Table 2. Station-wise dependence measures (or correlation coefficient) between annual maximum temperature and corresponding low flow

Station no	Pearson (r)	Kendall's tau (τ)	Spearman rho (ρ)	Overall correlation summary (measured at a 5% significance level)
2044	-0.7488514 (p-value = 1.132e-10)	-0.4758448 (p-value = 5.041e-07)	-0.6378389 (p-value = 2.792e-07)	Significant correlation exhibited

2084	0.3169008 (p-value = 0.03189)	-0.3588009 (p-value = 0.0004431)	-0.4746515 (p-value = 0.0008597)	Significant correlation exhibited
2106	-0.7400646 (p-value = p-value = 1.848e-09)	-0.5565913 (p-value = 2.497e-08)	-0.7193106 (p-value = 8.425e-09)	Significant correlation exhibited
2415	-0.2339408 (p-value = 0.1264)	-0.2330514 (p-value = 0.02604)	-0.3500969 (p-value = 0.01982)	Significant correlation exhibited
2473	-0.6197587 (p-value = 5.557e-05)	-0.4063492 (p-value = 0.0003698)	-0.5634492 (p-value = 0.0004336)	Significant correlation exhibited

Table 3. Estimation of copula dependence parameters via MPL estimator and their fitness test statistics in the bivariate joint dependence for (a) station 2044 (b) station 2084 (c) station 2106 (d) station 2415 (e) 2473

Copula function (station 2044) (a)	Estimated dependence parameter via Maximum pseudo likelihood (MPL) estimation	Cramer von Mises functional test statistics $\boldsymbol{S_n}$ (estimated p-value≥0.05) with parametric bootstrap procedure, (No. of Bootstrapping samples, N=1000)	
		S_n	p-value
Normal copula	rho.1 -0.7181	0.035244	0.2792
Frank copula	alpha -5.456	0.035917	0.1543
BB1 copula	theta delta 8.781e-08 1.000e+00	0.18702	0.002498
BB6 copula	theta delta 1 1	0.18702	0.001499
BB7 copula	theta delta 1.001e+00 1.265e-08	0.18754	0.001499
BB8 copula	theta delta 1 1	0.18702	0.0004995
rotated Clayton copula (90 degrees) *	**theta** **-1.567**	**0.020302**	**0.7238**
rotated Gumbel Copula (90 degrees)	theta -1.956	0.0341	0.3891

rotated Joe Copula (90 degrees)	theta -2.231	0.033872	0.4101
rotated BB1 Copula (90 degrees)	theta delta -0.7007 -1.5242	0.032562	-1.5242
rotated BB6 Copula (90 degrees)	theta delta -1 -1	0.18702	0.0004995
rotated BB7 Copula (90 degrees)	theta delta -1.808 -1.313	0.029089	0.478
rotated BB8 Copula (90 degrees)	theta delta -1 -1	0.18702	0.0004995
rotated Tawn type 1 Copula (90 degrees)	param1 param2 -1.956 1.000	0.0341	0.3561
rotated BB1 Copula (270 degrees)	theta delta -0.3902 -1.7228	0.033697	0.3821
rotated BB6 Copula (270 degrees)	theta delta -1 -1	0.18702	0.0004995
rotated BB7 Copula (270 degrees)	theta delta -2.062 -1.017	0.029559	0.482
rotated BB8 Copula (270 degrees)	theta delta -3.1385 -0.9258	0.027021	0.518

Note: rotated Clayton copula (90 degrees) (indicated by bold letter with an asterisk) exhibits minimum value of S_n fitness test statistics with p-value is greater than 0.05. Thus, it is recognized as the most parsimonious copula in defining bivariate joint dependence structure of the annual maximum temperature and corresponding low flow series for station 2044.

Copula function (station 2084) (b)	Estimated dependence parameter via Maximum pseudo likelihood (MPL) estimation	Cramer von Mises functional test statistics S_n (estimated p-value≥0.05) with parametric bootstrap procedure, (No. of Bootstrapping samples, N=1000)	
		S_n	p-value

Normal copula	rho.1 -0.5488	0.023322	0.9436
Frank copula	alpha -3.646	0.02445	0.8057
BB1 copula	theta delta 1.03e-08 1.00e+00	0.084469	0.05844
BB6 copula	theta delta 1 1	0.084469	0.08442
BB7 copula	theta delta 1.001e+00 8.281e-10	0.084792	0.06044
BB8 copula	theta delta 1 1	0.084469	0.07642
rotated Clayton copula (90 degrees)	theta -1.227	0.025779	0.6189
rotated Gumbel Copula (90 degrees)	theta -1.552	0.026197	0.6259
rotated Joe Copula (90 degrees)	theta -1.664	0.026679	0.5939
rotated BB1 Copula (90 degrees)	theta delta -0.9827 -1.1224	0.029269	0.526
rotated BB6 Copula (90 degrees)	theta delta -1 -1	0.084469	0.07343
rotated BB7 Copula (90 degrees)	theta delta -1.259 -1.133	0.030273	0.508
rotated BB8 Copula (90 degrees)	theta delta	0.084469	0.08941

	-1 -1		
rotated Tawn type 1 Copula (90 degrees)	param1 param2 -1.552 1.000	0.026197	0.6229
rotated BB1 Copula (270 degrees)	theta delta -4.927e-08 -1.669e+00	0.028352	0.526
rotated BB6 Copula (270 degrees)	theta delta -1 -1	0.084469	0.06543
rotated BB7 Copula (270 degrees)	theta delta -1.9375 -0.2999	0.026942	0.6159
rotated BB8 Copula (270 degrees) *	**theta delta** **-2.042 -1.000**	**0.022745**	**0.6948**
Note: rotated BB8 (270 degrees) (indicated by bold letter with an asterisk) exhibits minimum value of S_n goodness-of-fit test statistics with p-value is greater than 0.05. Thus, is recognized as the most parsimonious copula in defining bivariate joint dependence structure of the annual maximum temperature and corresponding low flow series for station 2084.			

Copula function (station 2106) (c)	Estimated dependence parameter via Maximum pseudo likelihood (MPL) estimation	Cramer von Mises functional test statistics S_n (estimated p-value≥0.05) with parametric bootstrap procedure, (No. of Bootstrapping samples, N=1000)	
		S_n	P-value
Normal copula	rho.1 -0.7881	0.033906	0.3402
Frank copula	alpha -6.713	0.033206	0.2622
BB1 copula	theta delta 6.603e-05 1.000e+00	0.26123	0.0004995

BB6 copula	theta delta 1 1	0.26119	0.0004995
BB7 copula	theta delta 1.001e+00 2.396e-09	0.26175	0.0004995
BB8 copula	theta delta 1 1	0.26119	0.0004995
rotated Clayton copula (90 degrees)	theta -1.837	0.048143	0.2273
rotated Gumbel Copula (90 degrees)	theta -2.335	0.026637	0.543
rotated Joe Copula (90 degrees) *	**theta** **-2.879**	**0.014513**	**0.8986**
rotated BB1 Copula (90 degrees)	theta delta -0.4211 -1.9909	0.033118	0.3981
rotated BB6 Copula (90 degrees)	theta delta -1 -1	0.26119	0.0004995
rotated BB7 Copula (90 degrees)	theta delta -2.499 -1.36	0.030011	0.4441
rotated BB8 Copula (90 degrees)	theta delta -3.6917 -0.9434	0.021281	0.6748
rotated Tawn type 1 Copula (90 degrees)	param1 param2 -2.4798 0.9345	0.025309	0.5699
rotated BB1 Copula (270 degrees)	theta delta -0.8344 -1.6955	0.030701	0.4451
rotated BB6 Copula (270 degrees)	theta delta	0.26119	0.0004995

	-1 -1		
rotated BB7 Copula (270 degrees)	theta delta -2.059 -1.813	0.027627	0.501
rotated BB8 Copula (270 degrees)	theta delta -1 -1	0.26119	0.0004995
Note: rotated Joe Copula (90 degrees) (indicated by bold letter with an asterisk) exhibits minimum value of S_n test statistics with p-value is greater than 0.05. Thus, it is recognized as the most parsimonious copula in defining bivariate joint dependence structure of the Annual maximum of temperature and corresponding low flow series for station 2106.			

Copula function (station 2415) (d)	Estimated dependence parameter via Maximum pseudo likelihood (MPL) estimation	Cramer von Mises functional test statistics S_n (estimated p-value≥0.05) with parametric bootstrap procedure, (No. of Bootstrapping samples, N=1000)	
		S_n	P-value
Normal copula	rho.1 -0.3787	0.032375	0.6758
Frank copula	alpha -2.109	0.027595	0.6818
BB1 copula	theta delta 2.088e-08 1.000e+00	0.034998	0.452
BB6 copula	theta delta 1 1	0.034998	0.472
BB7 copula	theta delta 1.001e+00 1.265e-08	0.035096	0.452
BB8 copula	theta delta 1 1	0.034998	0.503

rotated Clayton copula (90 degrees)	theta -0.4456	0.026018	0.6528
rotated Gumbel Copula (90 degrees)	theta -1.252	0.025662	0.6528
rotated Joe Copula (90 degrees)	theta -1.34	0.024057	0.7158
rotated BB1 Copula (90 degrees)	theta delta -0.2004 -1.1569	0.027384	0.6449
rotated BB6 Copula (90 degrees)	theta delta -1 -1	0.034998	0.469
rotated BB7 Copula (90 degrees)	theta delta -1.1264 -0.3663	0.026699	0.6249
rotated BB8 Copula (90 degrees)	theta delta -1, -1	0.034998	0.479
rotated Tawn type 1 Copula (90 degrees) *	**param1 param2** **-3.2865 0.2403**	**0.02097**	**0.7717**
rotated BB1 Copula (270 degrees)	theta delta -0.3254 -1.0935	0.027111	0.6259
rotated BB6 Copula (270 degrees)	theta delta -1 -1	0.034998	0.486
rotated BB7 Copula (270 degrees)	theta delta -1.0558 -0.4402	0.026	0.6409
rotated BB8 Copula (270 degrees)	theta delta -1.445e+03 -1.458e-03	0.034998	0.474

Note: rotated Tawn type 1 Copula (90 degrees) (indicated by bold letter with an asterisk) exhibits minimum value of S_n test statistics with p-value is greater than 0.05. Thus, is recognized as the most parsimonious copula in defining bivariate joint dependence structure for station 2415

Copula function (station 2473) (e)	Estimated dependence parameter via Maximum pseudo likelihood (MPL) estimation	Cramer von Mises functional test statistics $\boldsymbol{S_n}$ (estimated p-value≥0.05) with parametric bootstrap procedure, (No. of Bootstrapping samples, N=1000)	
		S_n	P-value
Normal copula	rho.1 -0.6338	0.036379	0.5989
Frank copula	alpha -4.406	0.034964	0.458
BB1 copula	theta delta 1.907e-09 1.000e+00	0.073043	0.1384
BB6 copula	theta delta 1 1	0.073043	0.1284
BB7 copula	theta delta 1.001e+00 9.660e-10	0.073298	0.1244
BB8 copula	theta delta 1 1	0.073043	0.1324
rotated Clayton copula (90 degrees) *	**theta -1.171**	**0.022113**	**0.7677**
rotated Gumbel Copula (90 degrees)	theta -1.698	0.033831	0.488
rotated Joe Copula (90 degrees)	theta -1.913	0.029917	0.5719

rotated BB1 Copula (90 degrees)	theta delta -0.5274 -1.4049	0.034121	0.472
rotated BB6 Copula (90 degrees)	theta delta -1 -1	0.073043	0.1424
rotated BB7 Copula (90 degrees)	theta delta -1.5749 -0.9248	0.031777	0.542
rotated BB8 Copula (90 degrees)	theta delta -1.557e+03 -2.826e-03	0.073043	0.1414
rotated Tawn type 1 Copula (90 degrees)	param1 param2 -1.7 1.0	0.03399	0.499
rotated BB1 Copula (270 degrees)	theta delta -0.3084 -1.5394	0.034728	0.505
rotated BB6 Copula (270 degrees)	theta delta -1 -1	0.073043	0.1484
rotated BB7 Copula (270 degrees)	theta delta -1.7369 -0.7381	0.032103	0.53
rotated BB8 Copula (270 degrees)	theta delta -4.5752 -0.6822	0.032048	0.541
Note: rotated Clayton copula (90 degrees) (indicated by bold letter with an asterisk) exhibits minimum value of S_n goodness-of-fit test statistics with p-value is greater than 0.05. Thus, is recognized as the most parsimonious copula in defining bivariate joint dependence structure for station 2473			

Table 4. Comparison of univariate and bivariate return periods (RPs) for compound events for the various possible combination for extreme characteristic for (a) station 2044 (b) station 2084 (c) station 2106 (d) station 2415 (e) station 2473

(a) Station 2044								
RPs (years)	AEP (Annual Exceedance probability)	NEP (Non-Exceedance Probability)	Annual maximum temperature (℃)	Corresponding low flow (m^3/sec) (Specific discharge ($\frac{m^3}{sec}/km^2$))	Univariate RP (Annual Maximum of Temperature) (YEARS)	Univariate RP (Corresponding Low Flow) (YEARS)	OR-JRP, T_{XY}^{OR} (YEARS)	AND-JRP, T_{XY}^{AND} (YEARS)
2	0.5	0.5	25.08	14.73 (0.00862)	2.00	2.00	1.16	7.22
5	0.2	0.8	26.09	18.80 (0.01100)	5.00	5.00	2.53	239.50
10	0.1	0.9	26.67	21.17 (0.01238)	10.00	10.00	5.01	3234.15
20	0.05	0.95	27.23	23.35 (0.01366)	20.00	20.00	10.00	40983.61
30	0.033333	0.966667	27.53	24.60 (0.01439)	30.00	30.00	15.00	178571.43
50	0.02	0.98	27.92	26.13 (0.01529)	50.00	50.00	25.00	1111111.11
79	0.012658	0.987342	28.26	27.50 (0.01609)	79.00	79.00	39.50	10000000.01
100	0.01	0.99	28.43	28.20 (0.01650)	100.00	100.00	50.00	9999999.99

(b) STATION_2084								
RPs (years)	AEP (Annual Exceedance probabilities)	NEP (Non-Exceedance Probability)	Annual maximum temperature (℃)	Corresponding low flow (m^3/sec) (Specific discharge ($\frac{m^3}{sec}/km^2$))	Univariate RP (Annual Maximum of Temperature) (YEARS)	Univariate RP (Corresponding Low Flow) (YEARS)	OR-JRP, T_{XY}^{OR} (YEARS)	AND-JRP, T_{XY}^{AND} (YEARS)
2	0.5	0.5	18.50	8.24 (0.02618)	2.00	2.00	1.19	6.29
5	0.2	0.8	19.96	15.59 (0.04953)	5.00	5.00	2.55	118.93
10	0.1	0.9	20.72	21.75 (0.06910)	10.00	10.00	5.02	1041.78

20	0.05	0.95	21.34	28.63 (0.09096)	20.00	20.00	10.01	8826.13
30	0.033333	0.966667	21.67	33.04 (0.10497)	30.00	30.00	15.01	30581.04
50	0.02	0.98	22.05	39.02 (0.12397)	50.00	50.00	25.00	147058.82
79	0.012658	0.987342	22.36	44.82 (0.14239)	79.00	79.00	39.50	588235.29
100	0.01	0.99	22.52	47.97 (0.15240)	100.00	100.00	50.00	1111111.11

(c)				STATION_2106				
RPs (years)	AEP (Annual Exceedance probabilities)	NEP (Non-Exceedance Probability)	Annual maximum temperature (℃)	Corresponding low flow ($\mathrm{m^3/sec}$) (Specific discharge ($\frac{\mathrm{m^3}}{\mathrm{sec}}/\mathrm{km^2}$))	Univariate RP (Annual Maximum of Temperature) (YEARS)	Univariate RP (Corresponding Low Flow) (YEARS)	OR-JRP, $\mathrm{T_{XY}^{OR}}$ (YEARS)	AND-JRP, $\mathrm{T_{XY}^{AND}}$ (YEARS)
2	0.5	0.5	21.70	4.34 (0.00460)	2.00	2.00	1.14	8.28
5	0.2	0.8	22.66	5.76 (0.00611)	5.00	5.00	2.52	412.05
10	0.1	0.9	23.22	6.70 (0.00711)	10.00	10.00	5.00	6830.60
20	0.05	0.95	23.74	7.60 (0.00806)	20.00	20.00	10.00	106382.98
30	0.033333	0.966667	24.03	8.11 (0.00860)	30.00	30.00	15.00	526315.79
50	0.02	0.98	24.39	8.76 (0.00929)	50.00	50.00	25.00	5000000.00
79	0.012658	0.987342	24.72	9.34 (0.00991)	79.00	79.00	39.50	Inf
100	0.01	0.99	24.88	9.63 (0.01021)	100.00	100.00	50.00	Inf

(d)				STATION_2415				
RPs (years)	AEP (Annual Exceedance probabilities)	NEP (Non-Exceedance Probability)	Annual maximum temperature (℃)	Corresponding low flow ($\mathrm{m^3/sec}$) (Specific discharge ($\frac{\mathrm{m^3}}{\mathrm{sec}}/km^2$))	Univariate RP (Annual Maximum of Temperature) (YEARS)	Univariate RP (Corresponding Low Flow) (YEARS)	OR-JRP, $\mathrm{T_{XY}^{OR}}$ (YEARS)	AND-JRP, $\mathrm{T_{XY}^{AND}}$ (YEARS)
2.00	0.50	0.50	24.60	4.76 (0.01139)	2.00	2.00	1.26	4.87
5.00	0.20	0.80	25.28	6.18 (0.01479)	5.00	5.00	2.71	32.06

10.00	0.10	0.90	25.67	7.07 (0.01692)	10.00	10.00	5.20	130.00
20.00	0.05	0.95	26.02	7.88 (0.01886)	20.00	20.00	10.19	523.31
30.00	0.03	0.97	26.23	8.33 (0.01993)	30.00	30.00	15.19	1179.80
50.00	0.02	0.98	26.48	8.87 (0.02122)	50.00	50.00	25.19	3282.99
79.00	0.01	0.99	26.70	9.35 (0.02237)	79.00	79.00	39.69	8203.45
100.00	0.01	0.99	26.82	9.58 (0.02292)	100.00	100.00	50.19	13140.60

(e)				STATION_2473				
RPs (years)	AEP (Annual Exceedance probabilities)	NEP (Non-Exceedance Probability)	Annual maximum temperature (℃)	Corresponding low flow ($\mathrm{m}^3/\mathrm{sec}$) (Specific discharge ($\frac{\mathrm{m}^3}{\mathrm{sec}}/\mathrm{km}^2$))	Univariate RP (Annual Maximum of Temperature) (YEARS)	Univariate RP (Corresponding Low Flow) (YEARS)	OR-JRP, $\mathrm{T}_{\mathrm{XY}}^{\mathrm{OR}}$ (YEARS)	AND-JRP, $\mathrm{T}_{\mathrm{XY}}^{\mathrm{AND}}$(YEARS)
2	0.5	0.5	16.54	178.26 (0.02830)	2.00	2.00	1.19	6.36
5	0.2	0.8	17.45	223.86 (0.03554)	5.00	5.00	2.55	134.52
10	0.1	0.9	17.98	252.16 (0.04003)	10.00	10.00	5.02	1332.98
20	0.05	0.95	18.47	278.21 (0.04417)	20.00	20.00	10.01	12642.23
30	0.033333	0.966667	18.75	292.82 (0.04649)	30.00	30.00	15.00	46728.97
50	0.02	0.98	19.09	310.77 (0.04933)	50.00	50.00	25.00	238095.24
79	0.012658	0.987342	19.40	326.52 (0.05184)	79.00	79.00	39.50	1111111.11
100	0.01	0.99	19.55	334.56 (0.05311)	100.00	100.00	50.00	2000000.00

List of Figures

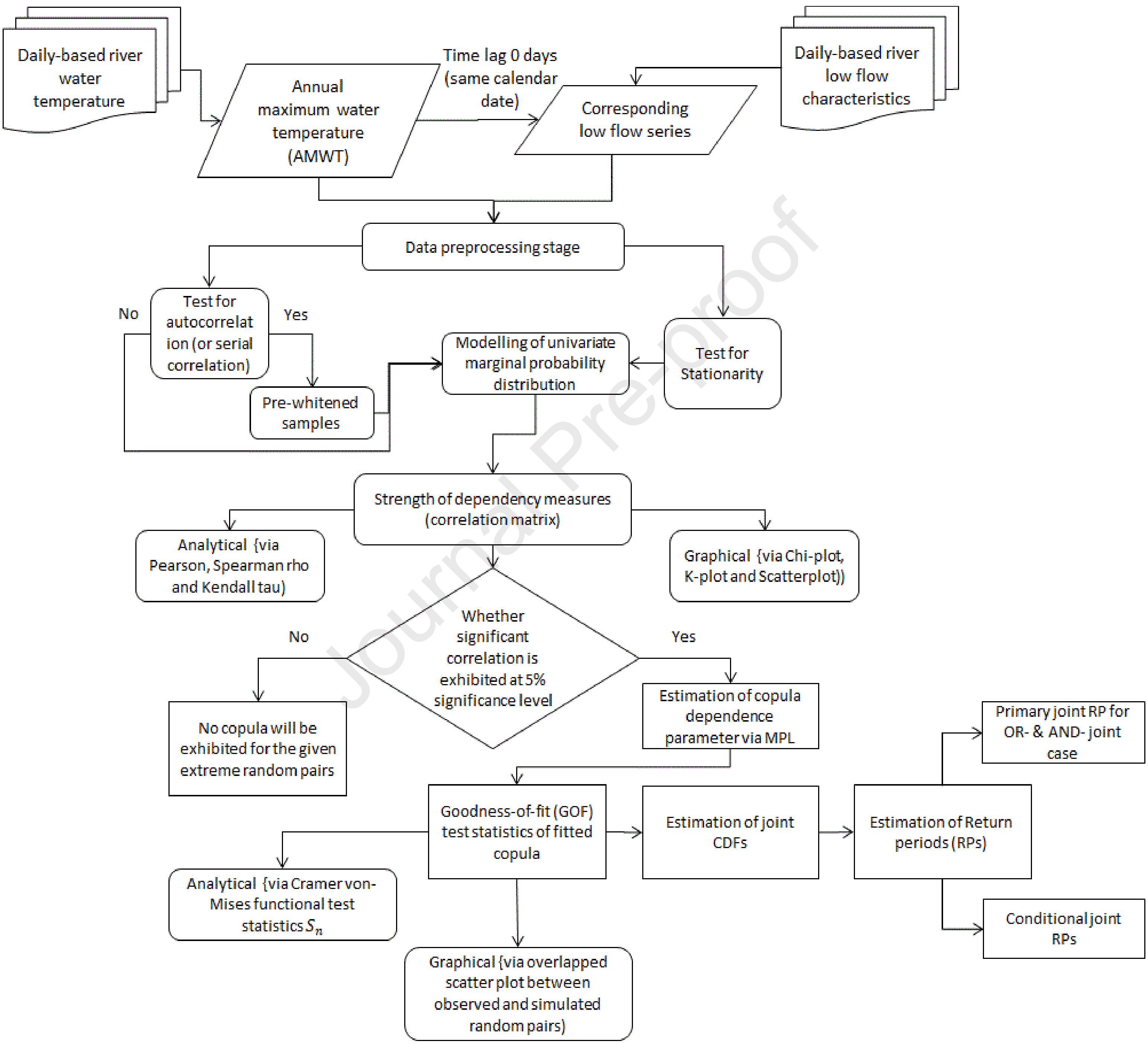

Figure 1. Methodological workflow in the bivariate joint modelling of annual maximum water temperature and corresponding low flow series

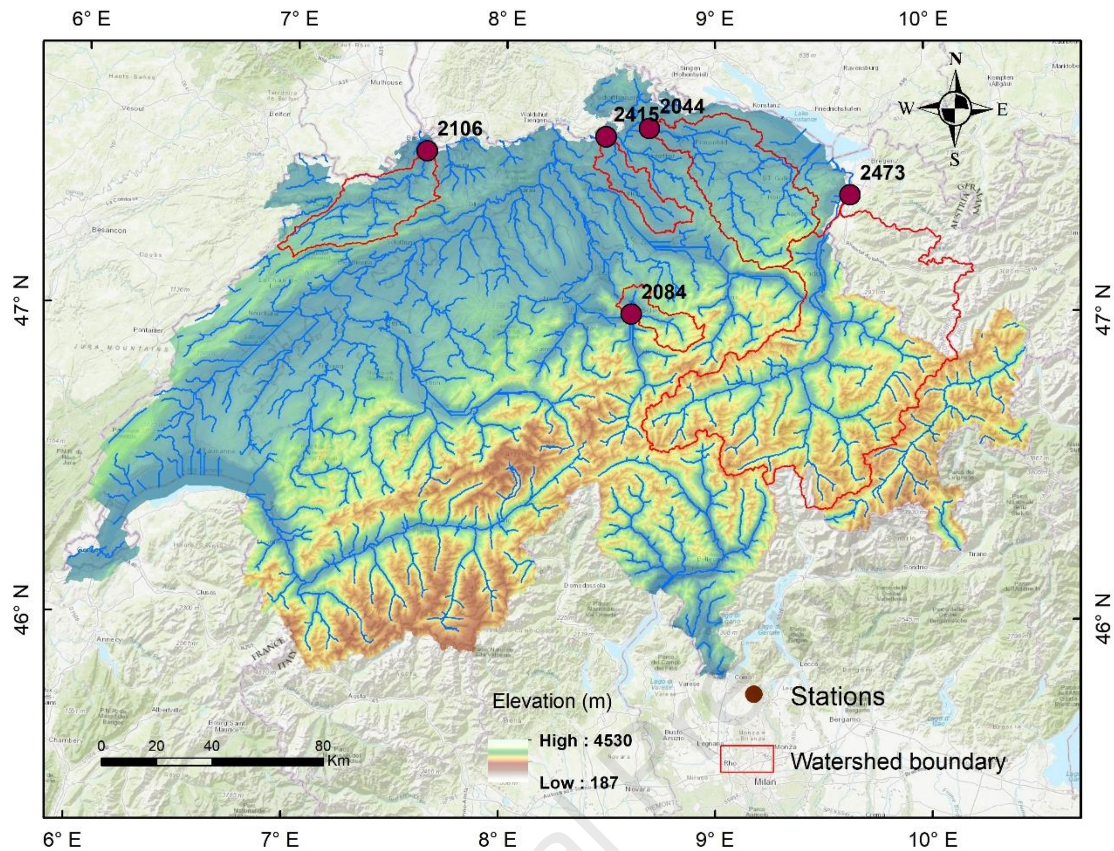

Figure 2. The geographical location of the study area

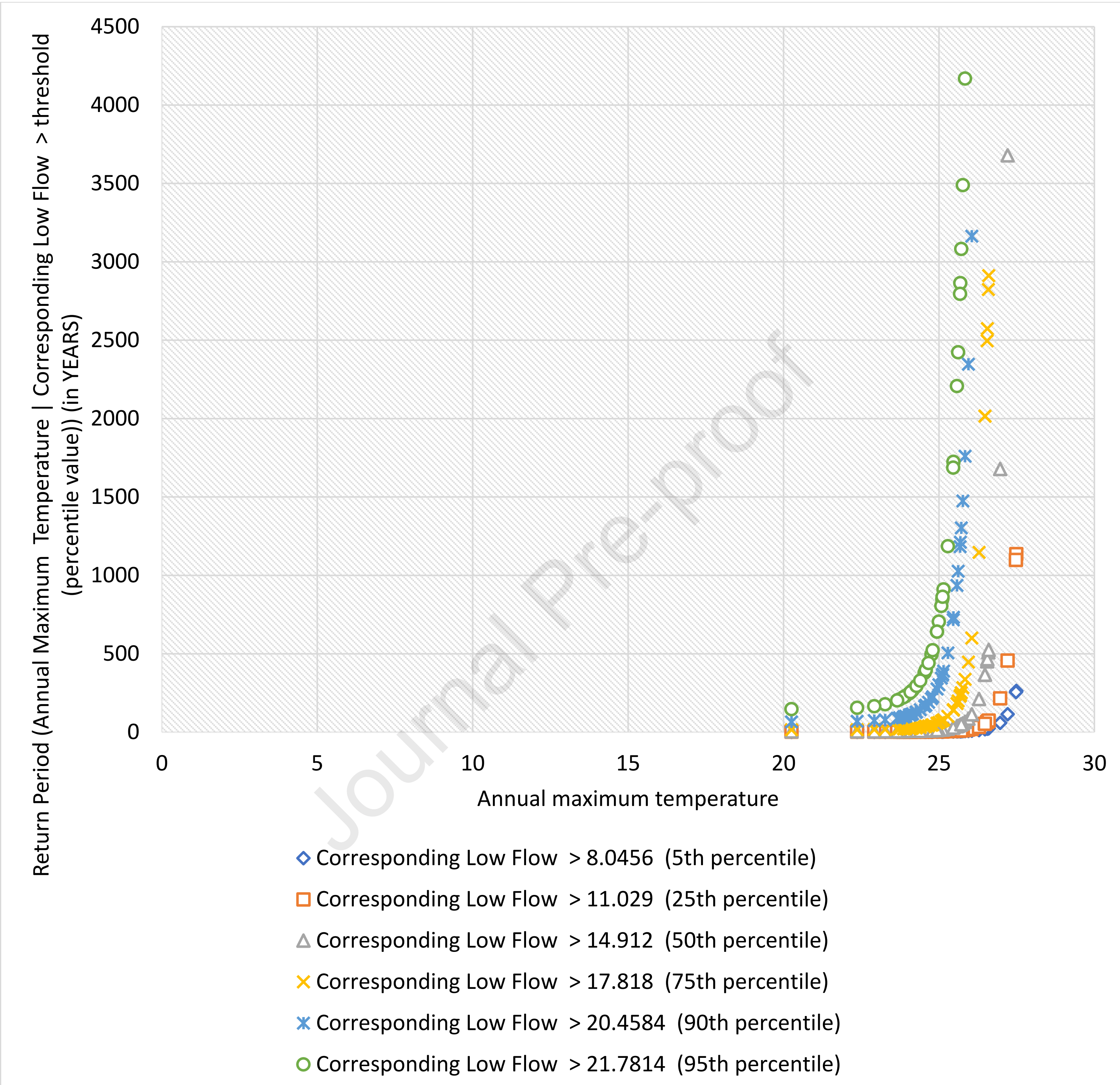
Return Period (Annual Maximum Temperature | Corresponding Low Flow > threshold (percentile value)) (in YEARS)
4500
4000
3500
3000
2500
2000
1500
1000
500
0
0
5
10
15
20
25
30
Annual maximum temperature
Corresponding Low Flow > 8.0456 (5th percentile)
Corresponding Low Flow > 11.029 (25th percentile)
Corresponding Low Flow > 14.912 (50th percentile)
Corresponding Low Flow > 17.818 (75th percentile)
Corresponding Low Flow > 20.4584 (90th percentile)
Corresponding Low Flow > 21.7814 (95th percentile)

(a)

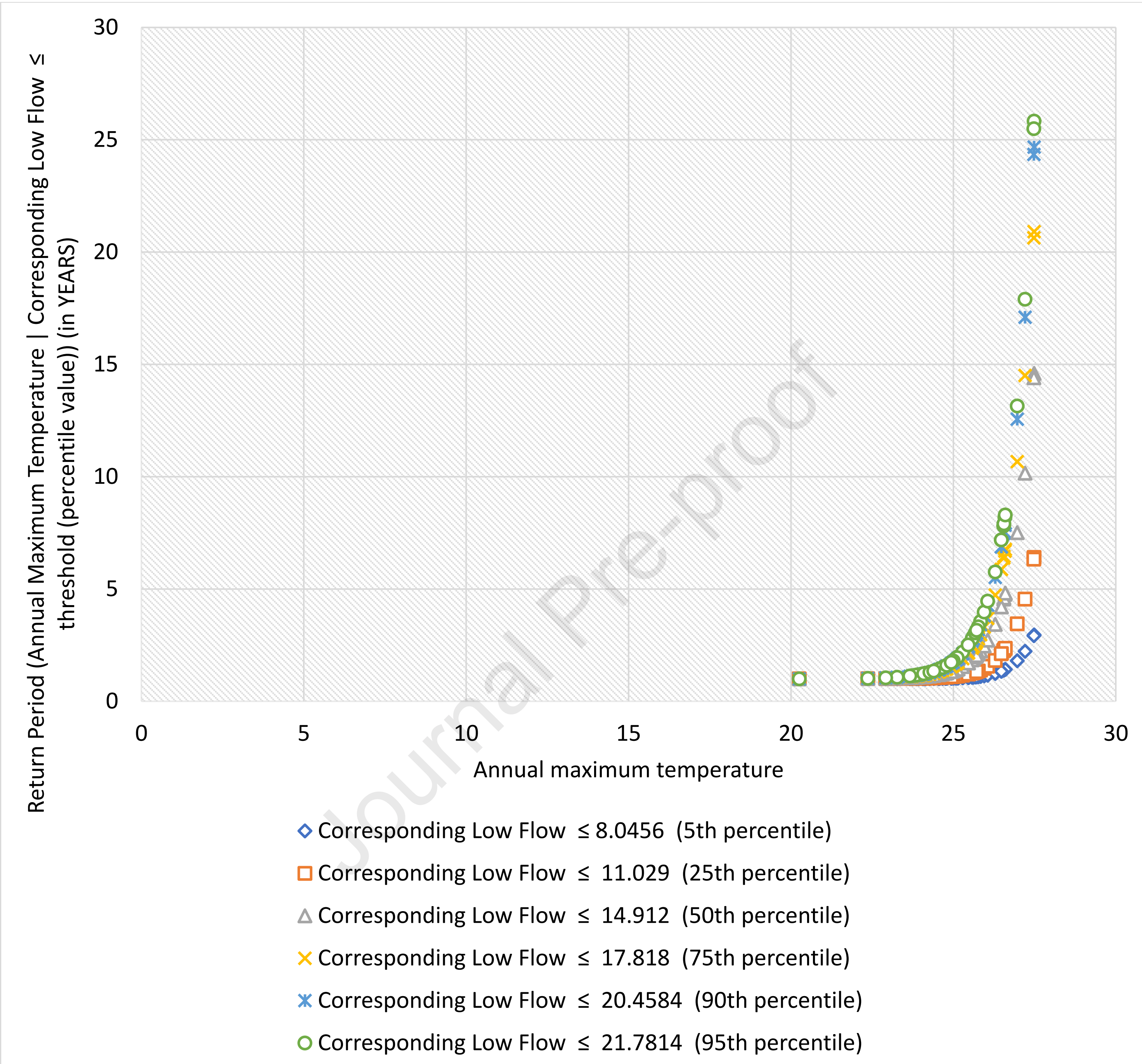

30
25
20
15
10
5
0
0
5
10
15
20
25
30
Annual maximum temperature
Return Period (Annual Maximum Temperature | Corresponding Low Flow ≤ threshold (percentile value)) (in YEARS)
Corresponding Low Flow ≤ 8.0456 (5th percentile)
Corresponding Low Flow ≤ 11.029 (25th percentile)
Corresponding Low Flow ≤ 14.912 (50th percentile)
Corresponding Low Flow ≤ 17.818 (75th percentile)
Corresponding Low Flow ≤ 20.4584 (90th percentile)
Corresponding Low Flow ≤ 21.7814 (95th percentile)

(b)

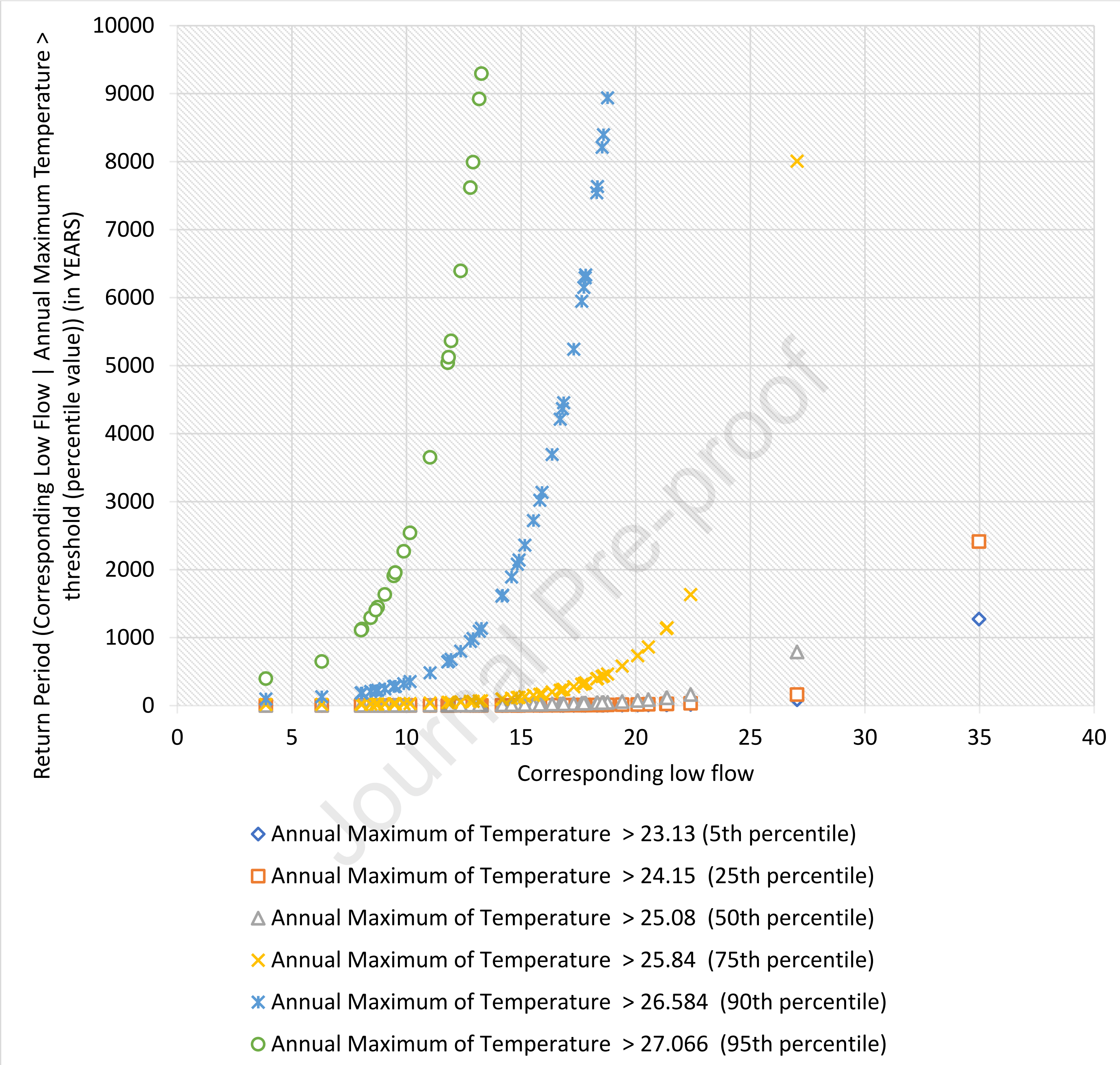
Return Period (Corresponding Low Flow | Annual Maximum Temperature > threshold (percentile value)) (in YEARS)
10000
9000
8000
7000
6000
5000
4000
3000
2000
1000
0
0
5
10
15
20
25
30
35
40
Corresponding low flow
Annual Maximum of Temperature > 23.13 (5th percentile)
Annual Maximum of Temperature > 24.15 (25th percentile)
Annual Maximum of Temperature > 25.08 (50th percentile)
Annual Maximum of Temperature > 25.84 (75th percentile)
Annual Maximum of Temperature > 26.584 (90th percentile)
Annual Maximum of Temperature > 27.066 (95th percentile)

(c)

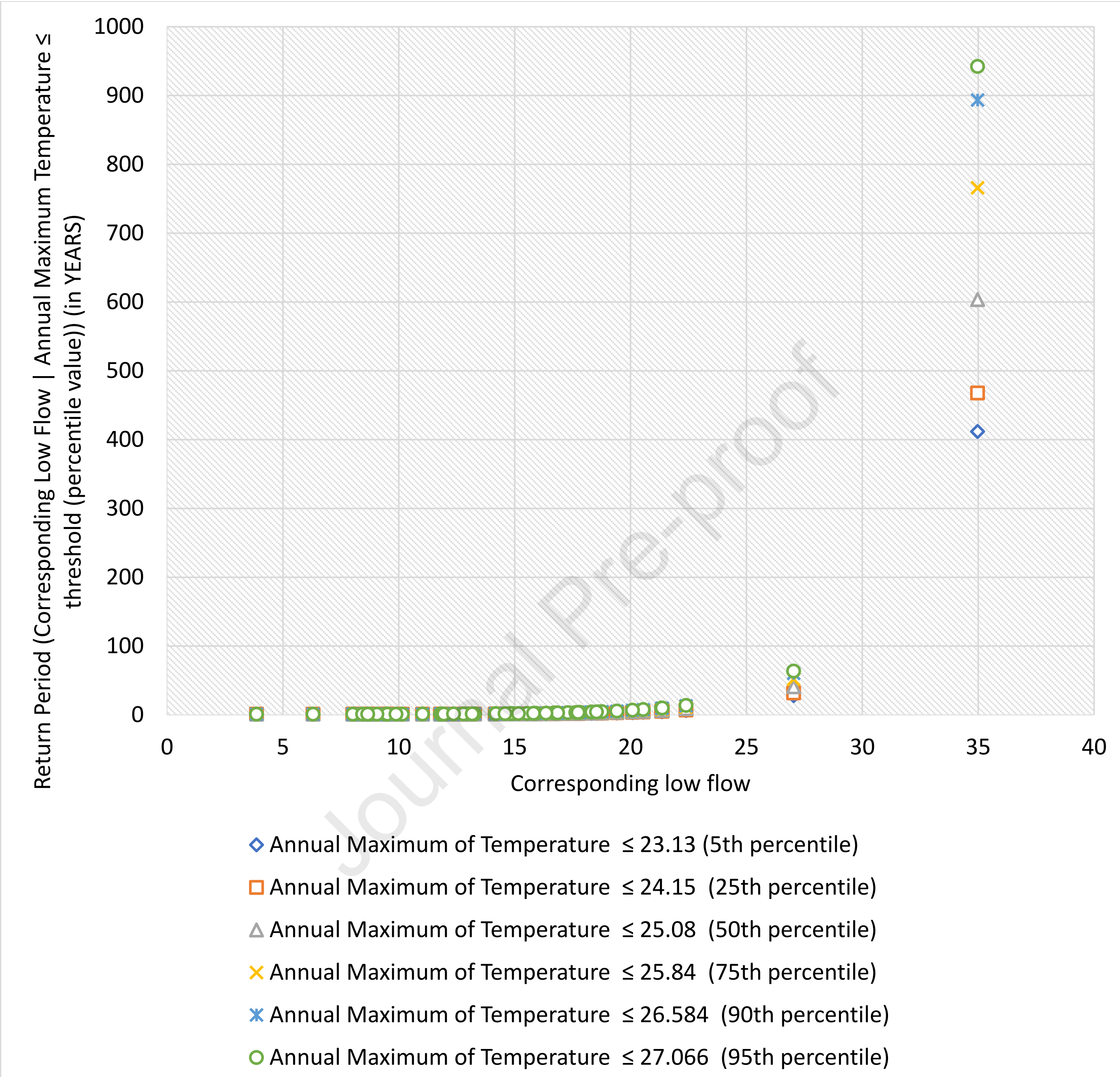

(d)

Figure 3. (a) Estimating the conditional joint return periods for station 2044 (a) for case Annual Maximum Temperature | Corresponding Low Flow > threshold (percentile value) (b) for case Annual Maximum Temperature | Corresponding Low Flow ≤ threshold (percentile value) (c) for case Corresponding Low Flow | Annual Maximum Temperature > threshold (percentile value) (d) for case, Corresponding Low Flow | Annual Maximum Temperature ≤ threshold (percentile value)).

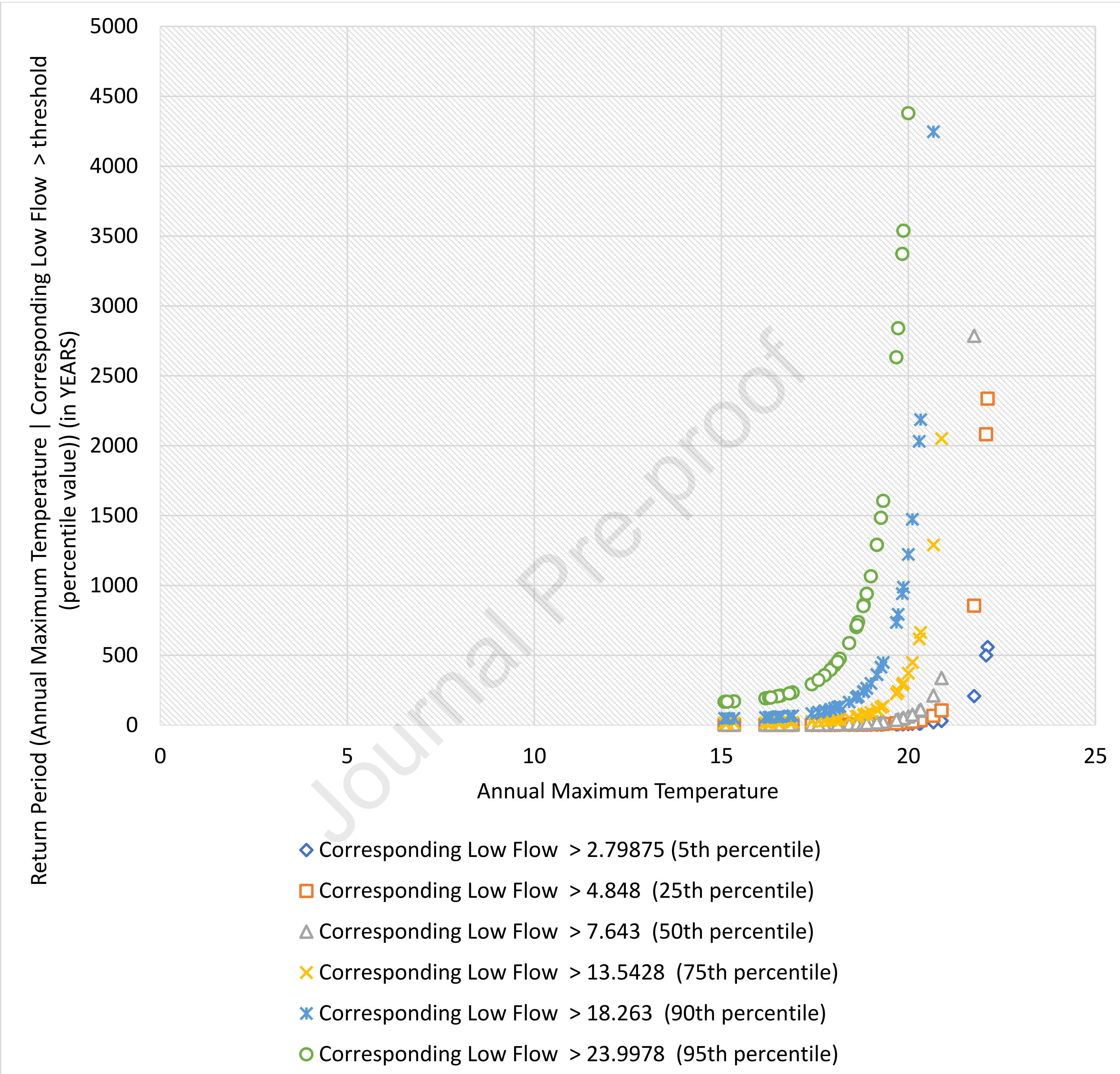
5000
4500
4000
3500
3000
2500
2000
1500
1000
500
0
0
5
10
15
20
25
Return Period (Annual Maximum Temperature | Corresponding Low Flow > threshold (percentile value)) (in YEARS)
Annual Maximum Temperature
Corresponding Low Flow > 2.79875 (5th percentile)
Corresponding Low Flow > 4.848 (25th percentile)
Corresponding Low Flow > 7.643 (50th percentile)
Corresponding Low Flow > 13.5428 (75th percentile)
Corresponding Low Flow > 18.263 (90th percentile)
Corresponding Low Flow > 23.9978 (95th percentile)

(a)

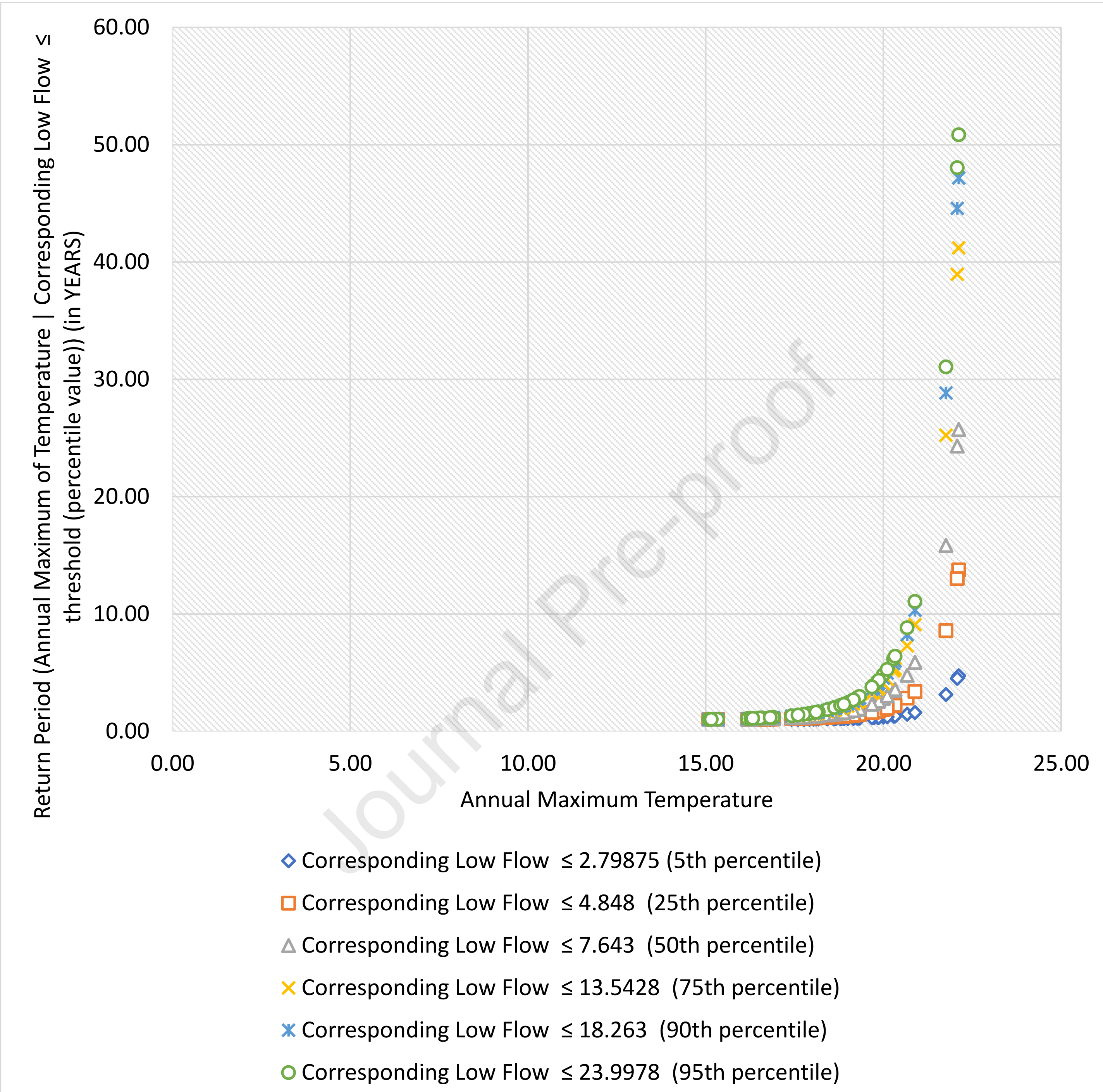

60.00
50.00
40.00
30.00
20.00
10.00
0.00
0.00
5.00
10.00
15.00
20.00
25.00
Return Period (Annual Maximum of Temperature | Corresponding Low Flow ≤ threshold (percentile value)) (in YEARS)
Annual Maximum Temperature
Corresponding Low Flow ≤ 2.79875 (5th percentile)
Corresponding Low Flow ≤ 4.848 (25th percentile)
Corresponding Low Flow ≤ 7.643 (50th percentile)
Corresponding Low Flow ≤ 13.5428 (75th percentile)
Corresponding Low Flow ≤ 18.263 (90th percentile)
Corresponding Low Flow ≤ 23.9978 (95th percentile)

(b)

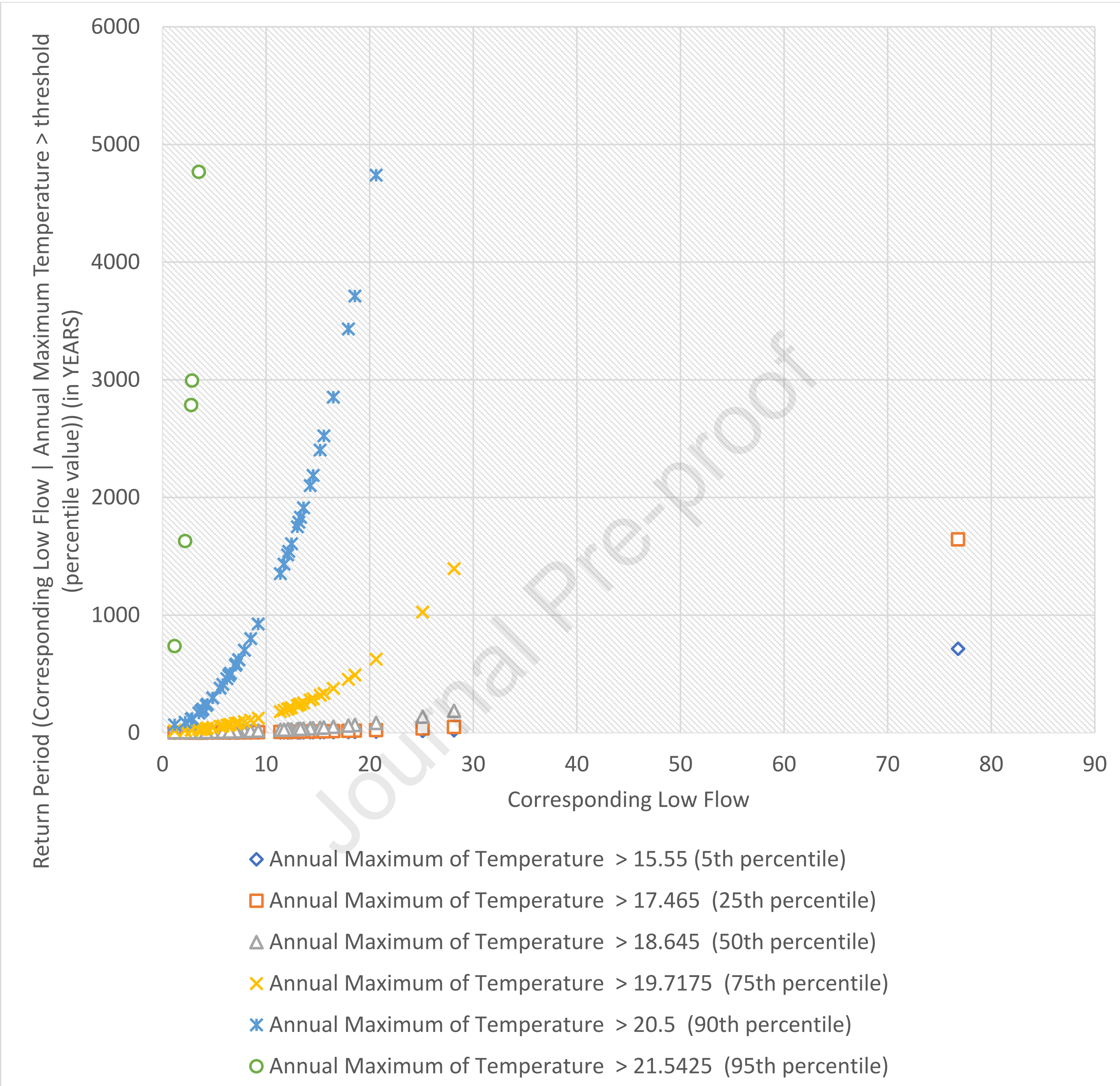

Return Period (Corresponding Low Flow | Annual Maximum Temperature > threshold (percentile value)) (in YEARS)
6000
5000
4000
3000
2000
1000
0
0
10
20
30
40
50
60
70
80
90
Corresponding Low Flow
Annual Maximum of Temperature > 15.55 (5th percentile)
Annual Maximum of Temperature > 17.465 (25th percentile)
Annual Maximum of Temperature > 18.645 (50th percentile)
Annual Maximum of Temperature > 19.7175 (75th percentile)
Annual Maximum of Temperature > 20.5 (90th percentile)
Annual Maximum of Temperature > 21.5425 (95th percentile)

(c)

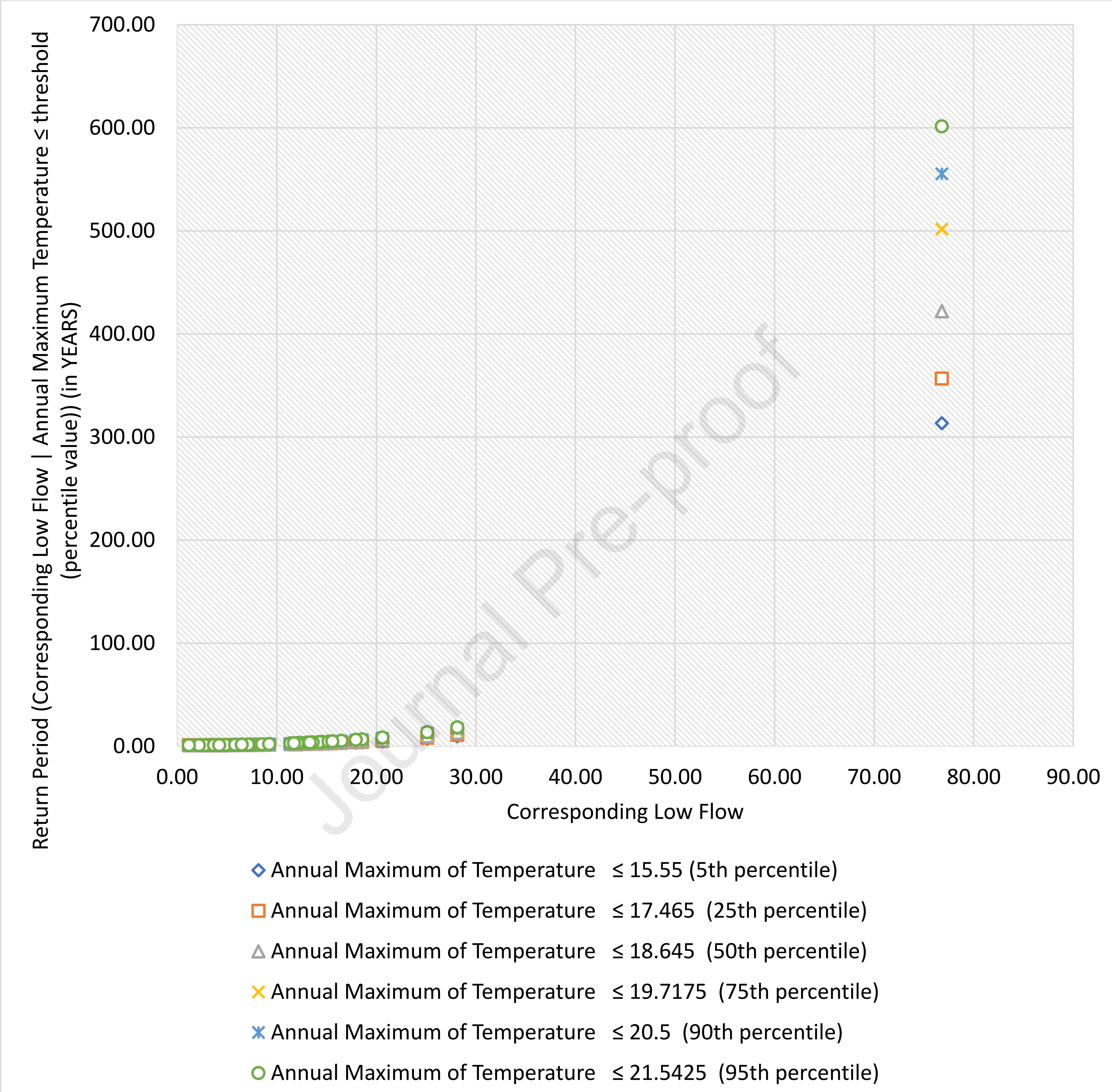

(d)

Figure 4. (a) Estimating the conditional joint return periods for station 2084 (a) for case, Annual Maximum Temperature | Corresponding Low Flow > threshold (percentile value) (b) for case, Annual Maximum Temperature | Corresponding Low Flow ≤ threshold (percentile value) (c) for

case, Corresponding Low Flow | Annual Maximum Temperature > threshold (percentile value) (d) for case, Corresponding Low Flow | Annual Maximum Temperature ≤ threshold (percentile value)).

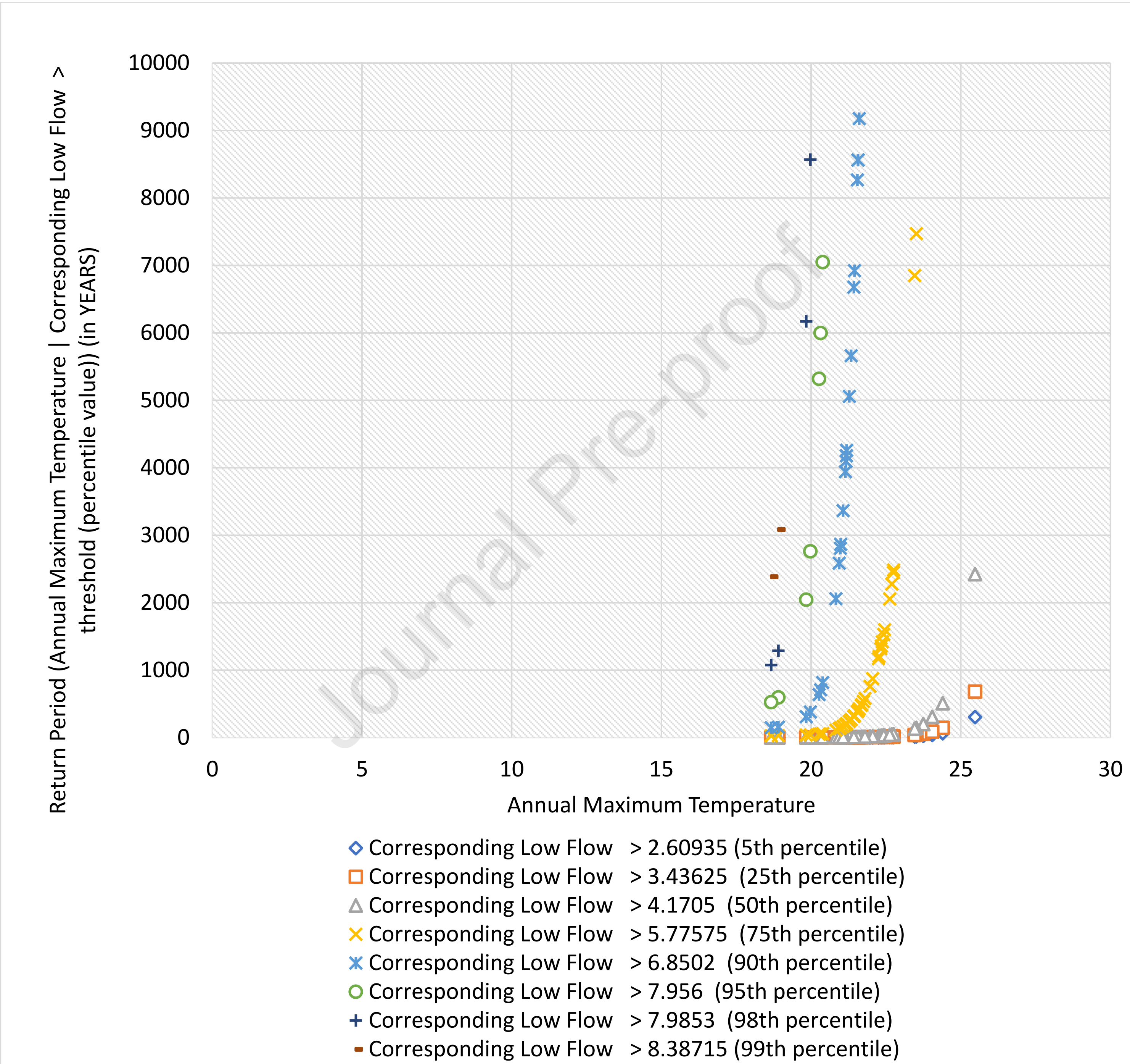

(a)

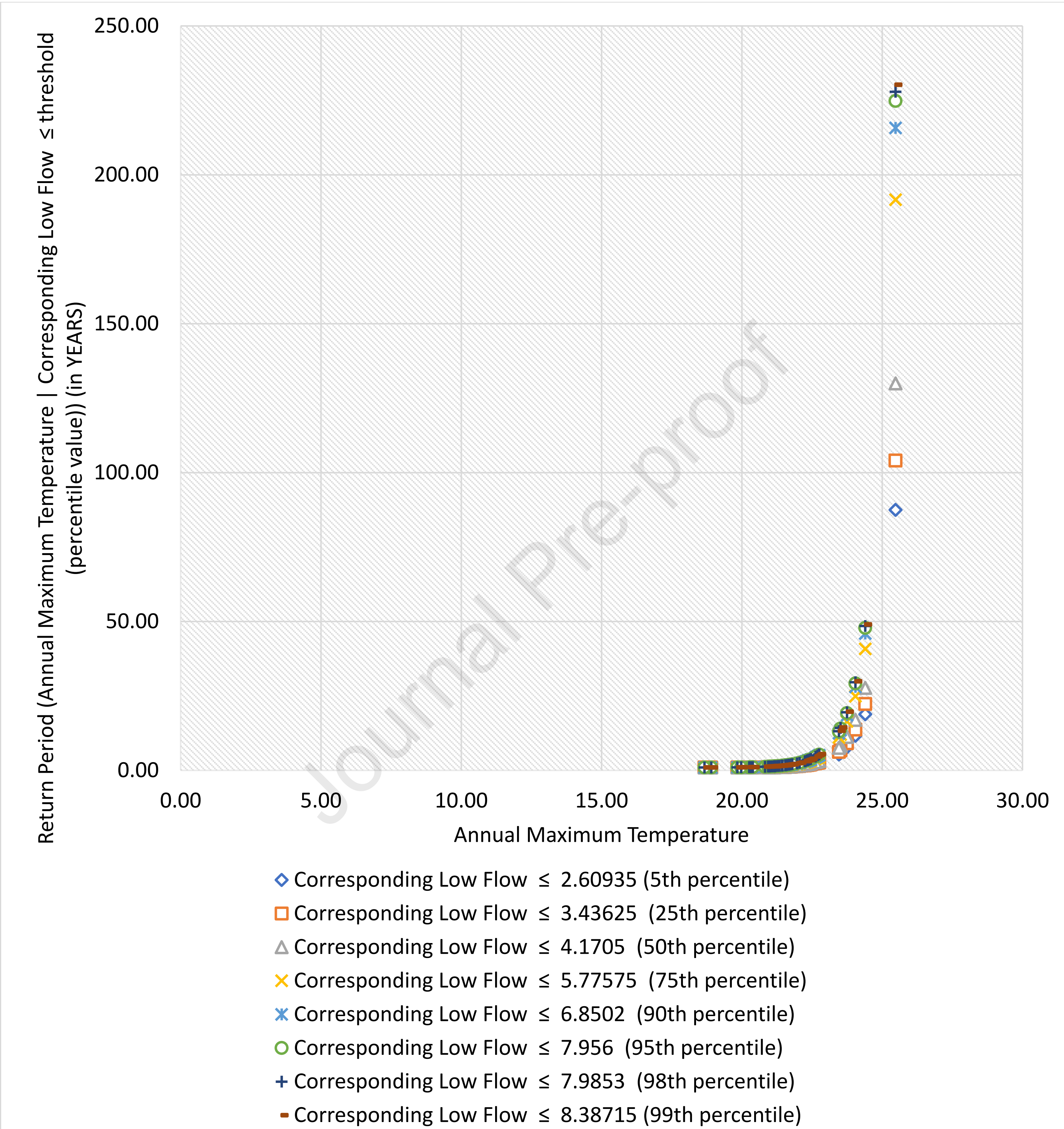

250.00
200.00
150.00
100.00
50.00
0.00
0.00
5.00
10.00
15.00
20.00
25.00
30.00
Return Period (Annual Maximum Temperature | Corresponding Low Flow ≤ threshold (percentile value)) (in YEARS)
Annual Maximum Temperature
Corresponding Low Flow ≤ 2.60935 (5th percentile)
Corresponding Low Flow ≤ 3.43625 (25th percentile)
Corresponding Low Flow ≤ 4.1705 (50th percentile)
Corresponding Low Flow ≤ 5.77575 (75th percentile)
Corresponding Low Flow ≤ 6.8502 (90th percentile)
Corresponding Low Flow ≤ 7.956 (95th percentile)
Corresponding Low Flow ≤ 7.9853 (98th percentile)
Corresponding Low Flow ≤ 8.38715 (99th percentile)

(b)

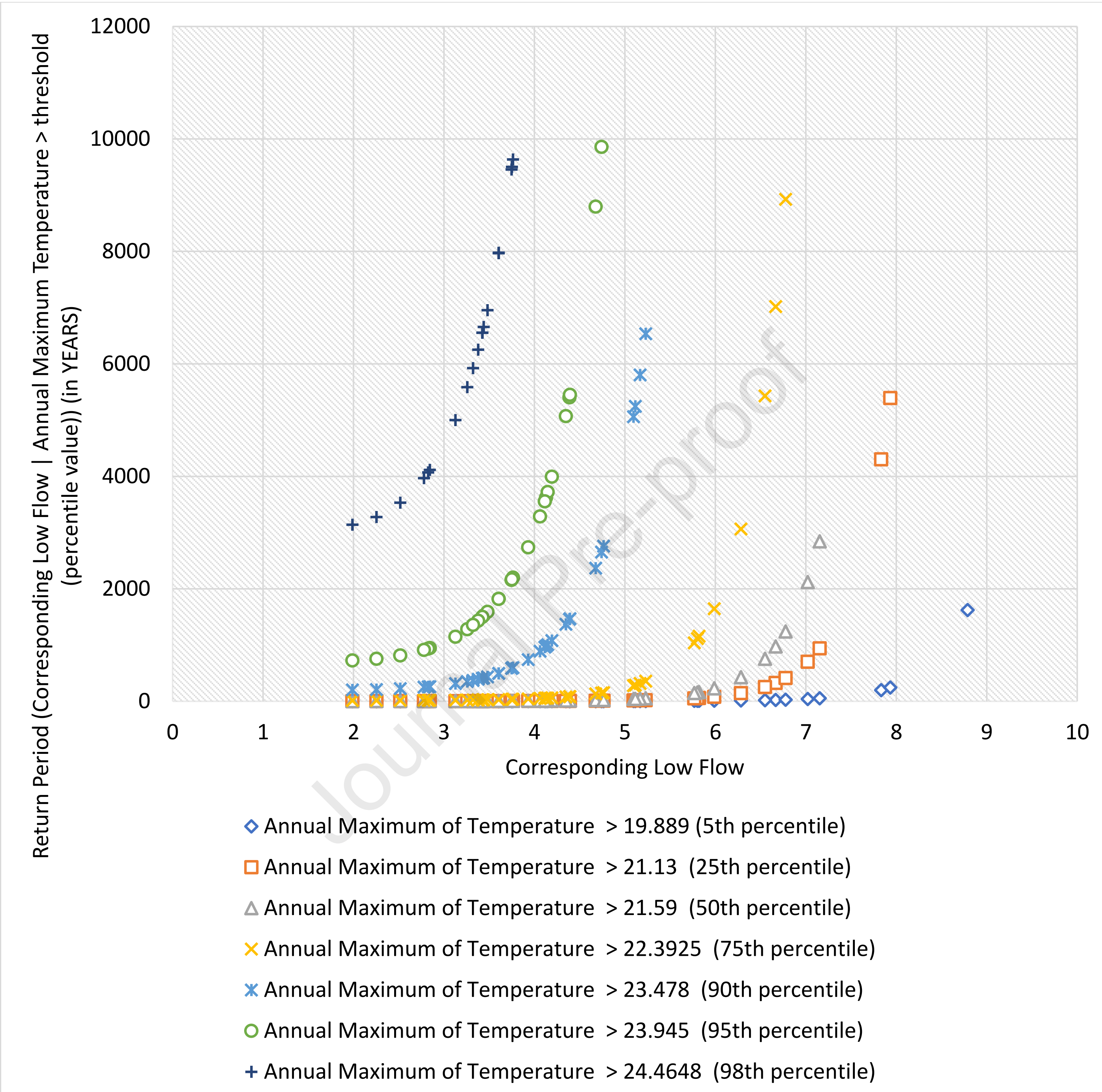

12000
10000
8000
6000
4000
2000
0
0
1
2
3
4
5
6
7
8
9
10
Return Period (Corresponding Low Flow | Annual Maximum Temperature > threshold (percentile value)) (in YEARS)
Corresponding Low Flow
Annual Maximum of Temperature > 19.889 (5th percentile)
Annual Maximum of Temperature > 21.13 (25th percentile)
Annual Maximum of Temperature > 21.59 (50th percentile)
Annual Maximum of Temperature > 22.3925 (75th percentile)
Annual Maximum of Temperature > 23.478 (90th percentile)
Annual Maximum of Temperature > 23.945 (95th percentile)
Annual Maximum of Temperature > 24.4648 (98th percentile)

(c)

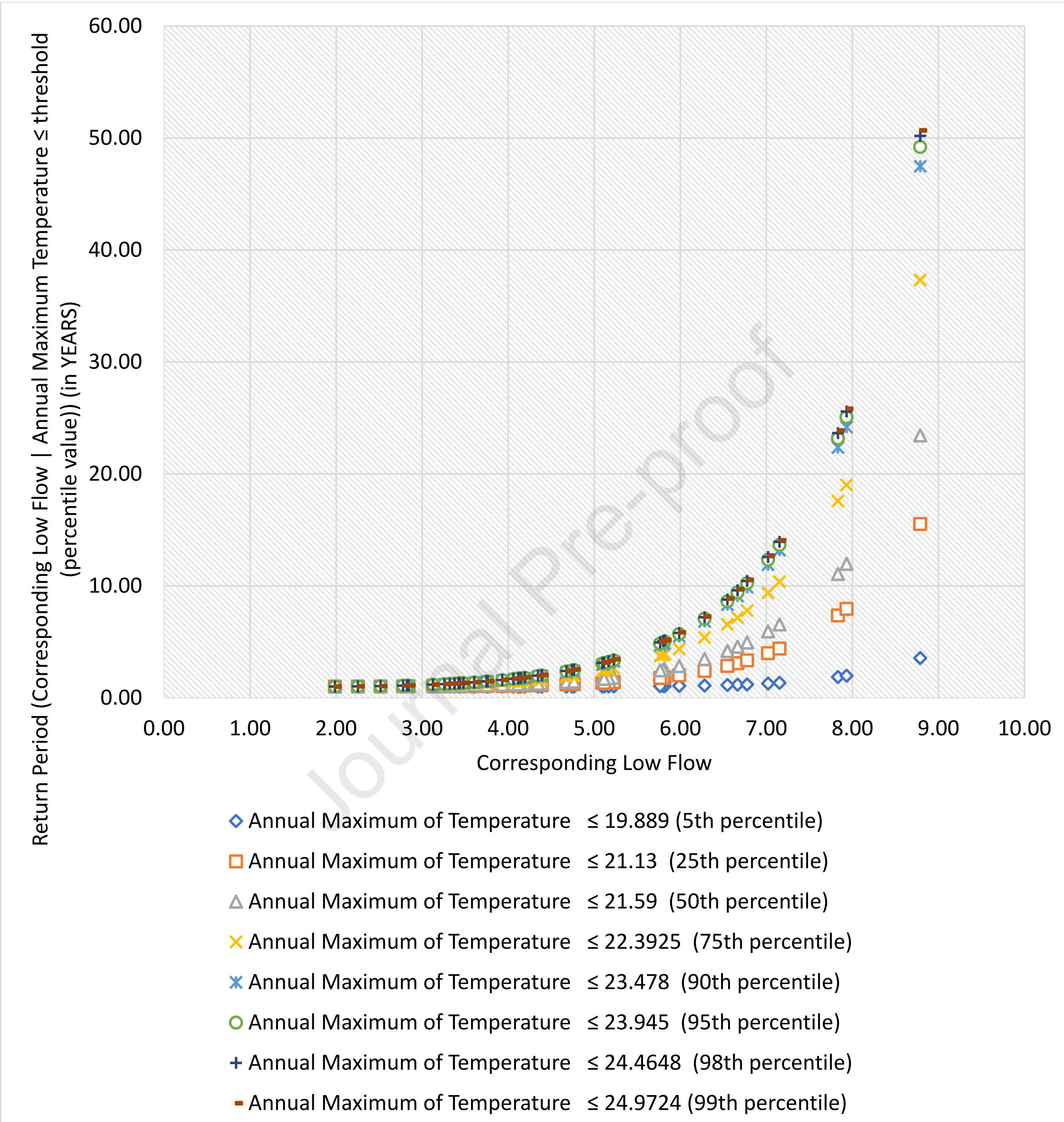

(d)

Figure 5. (a) Estimating the conditional joint return periods for station 2106 (a) for case, Annual Maximum Temperature | Corresponding Low Flow > threshold (percentile value) (b) for case, Annual Maximum Temperature | Corresponding Low Flow ≤ threshold (percentile value) (c) for

case, Corresponding Low Flow | Annual Maximum Temperature > threshold (percentile value) (d) for case, Corresponding Low Flow | Annual Maximum Temperature ≤ threshold (percentile value)).

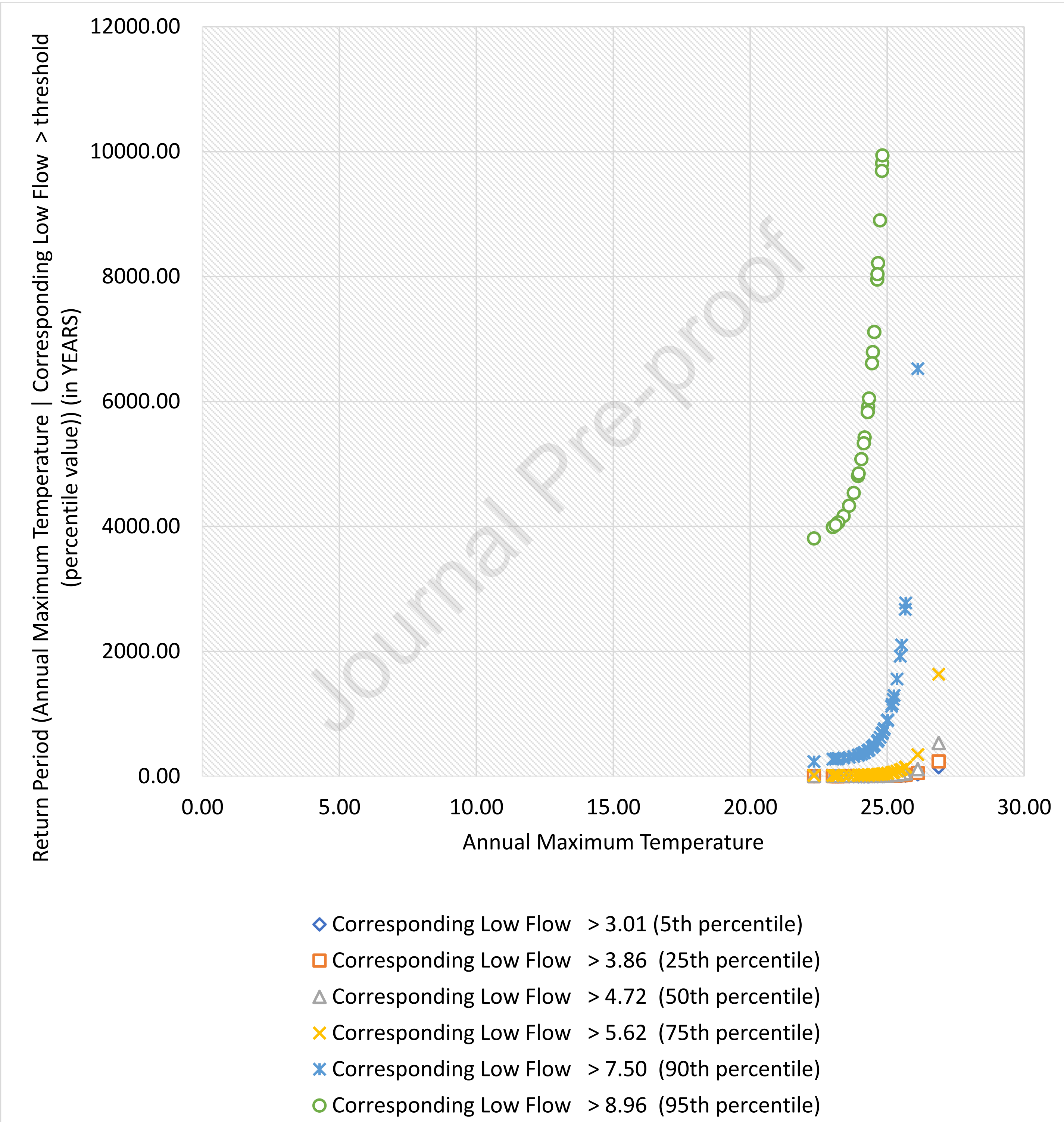

(a)

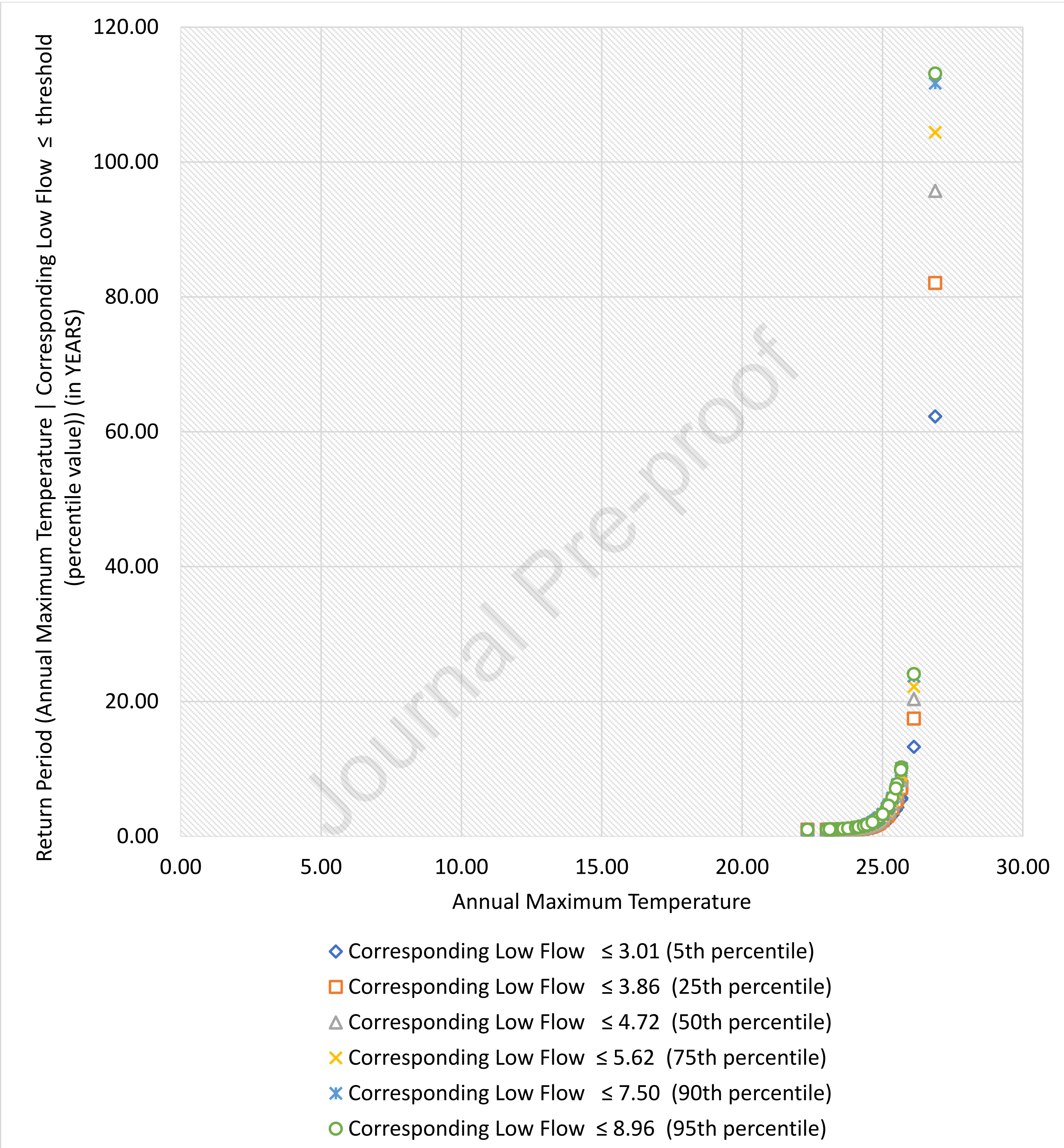

Return Period (Annual Maximum Temperature | Corresponding Low Flow ≤ threshold (percentile value)) (in YEARS)
120.00
100.00
80.00
60.00
40.00
20.00
0.00
0.00
5.00
10.00
15.00
20.00
25.00
30.00
Annual Maximum Temperature
Corresponding Low Flow ≤ 3.01 (5th percentile)
Corresponding Low Flow ≤ 3.86 (25th percentile)
Corresponding Low Flow ≤ 4.72 (50th percentile)
Corresponding Low Flow ≤ 5.62 (75th percentile)
Corresponding Low Flow ≤ 7.50 (90th percentile)
Corresponding Low Flow ≤ 8.96 (95th percentile)

(b)

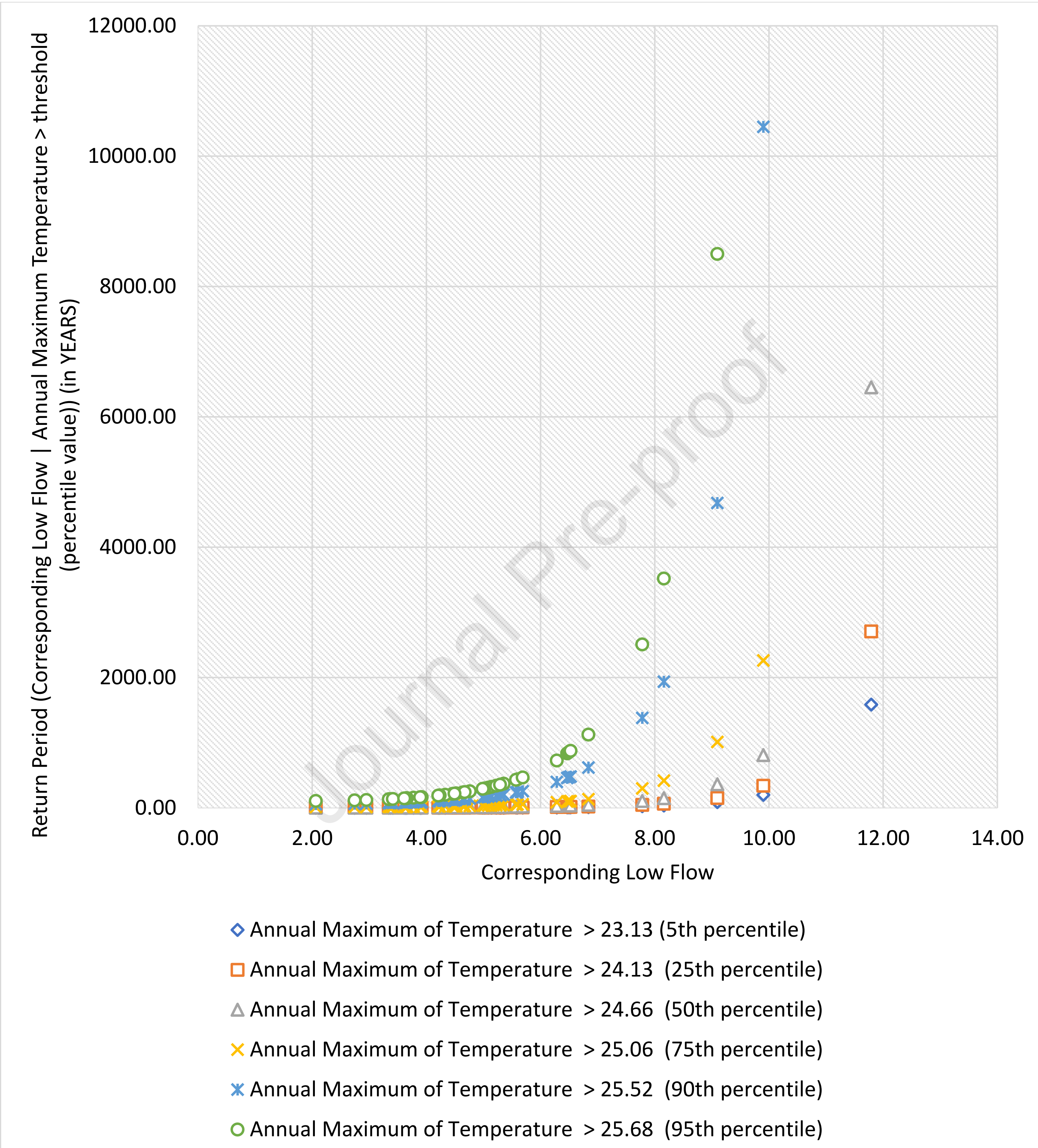

Return Period (Corresponding Low Flow | Annual Maximum Temperature > threshold (percentile value)) (in YEARS)
12000.00
10000.00
8000.00
6000.00
4000.00
2000.00
0.00
0.00
2.00
4.00
6.00
8.00
10.00
12.00
14.00
Corresponding Low Flow
Annual Maximum of Temperature > 23.13 (5th percentile)
Annual Maximum of Temperature > 24.13 (25th percentile)
Annual Maximum of Temperature > 24.66 (50th percentile)
Annual Maximum of Temperature > 25.06 (75th percentile)
Annual Maximum of Temperature > 25.52 (90th percentile)
Annual Maximum of Temperature > 25.68 (95th percentile)

(c)

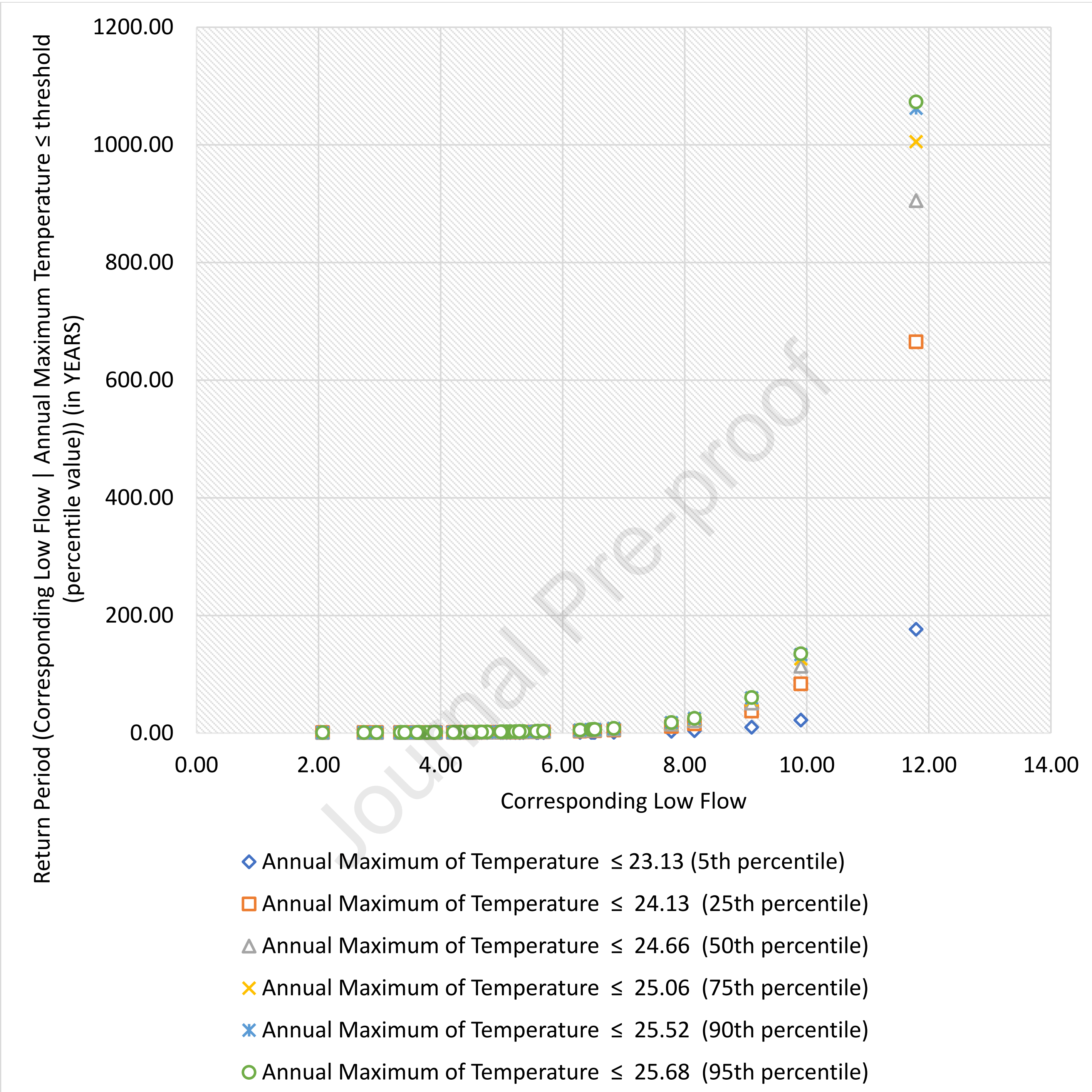

(d)

Figure 6. (a) Estimating the conditional joint return periods for station 2415 (a) for case, Annual Maximum Temperature | Corresponding Low Flow > threshold (percentile value) (b) for case, Annual Maximum Temperature | Corresponding Low Flow ≤ threshold (percentile value) (c) for case, Corresponding Low Flow | Annual Maximum Temperature > threshold (percentile value)

(d) for case, Corresponding Low Flow | Annual Maximum Temperature ≤ threshold (percentile value))

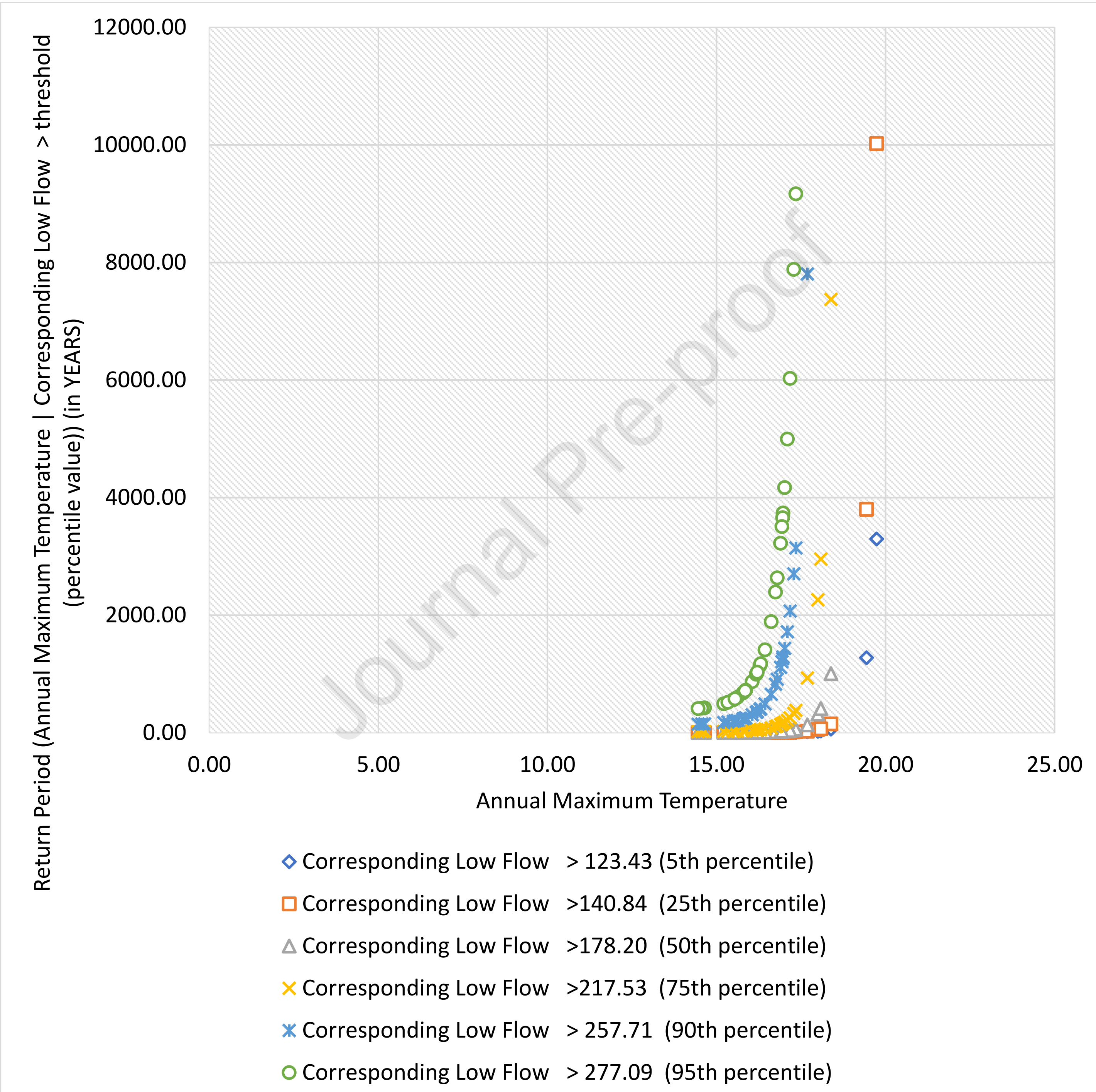

(a)

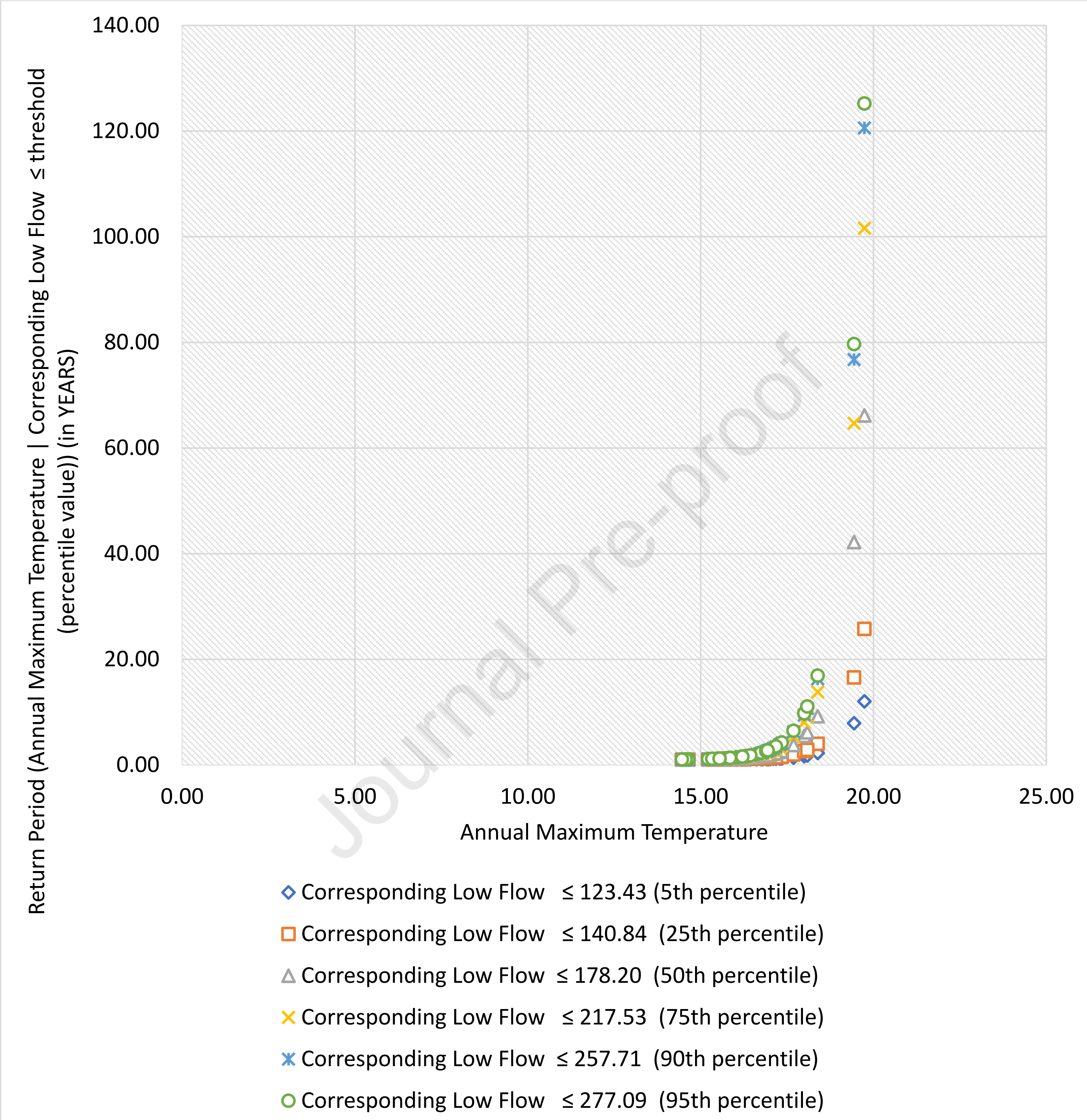

140.00
120.00
100.00
80.00
60.00
40.00
20.00
0.00
0.00
5.00
10.00
15.00
20.00
25.00
Return Period (Annual Maximum Temperature | Corresponding Low Flow ≤ threshold (percentile value)) (in YEARS)
Annual Maximum Temperature
Corresponding Low Flow ≤ 123.43 (5th percentile)
Corresponding Low Flow ≤ 140.84 (25th percentile)
Corresponding Low Flow ≤ 178.20 (50th percentile)
Corresponding Low Flow ≤ 217.53 (75th percentile)
Corresponding Low Flow ≤ 257.71 (90th percentile)
Corresponding Low Flow ≤ 277.09 (95th percentile)

(b)

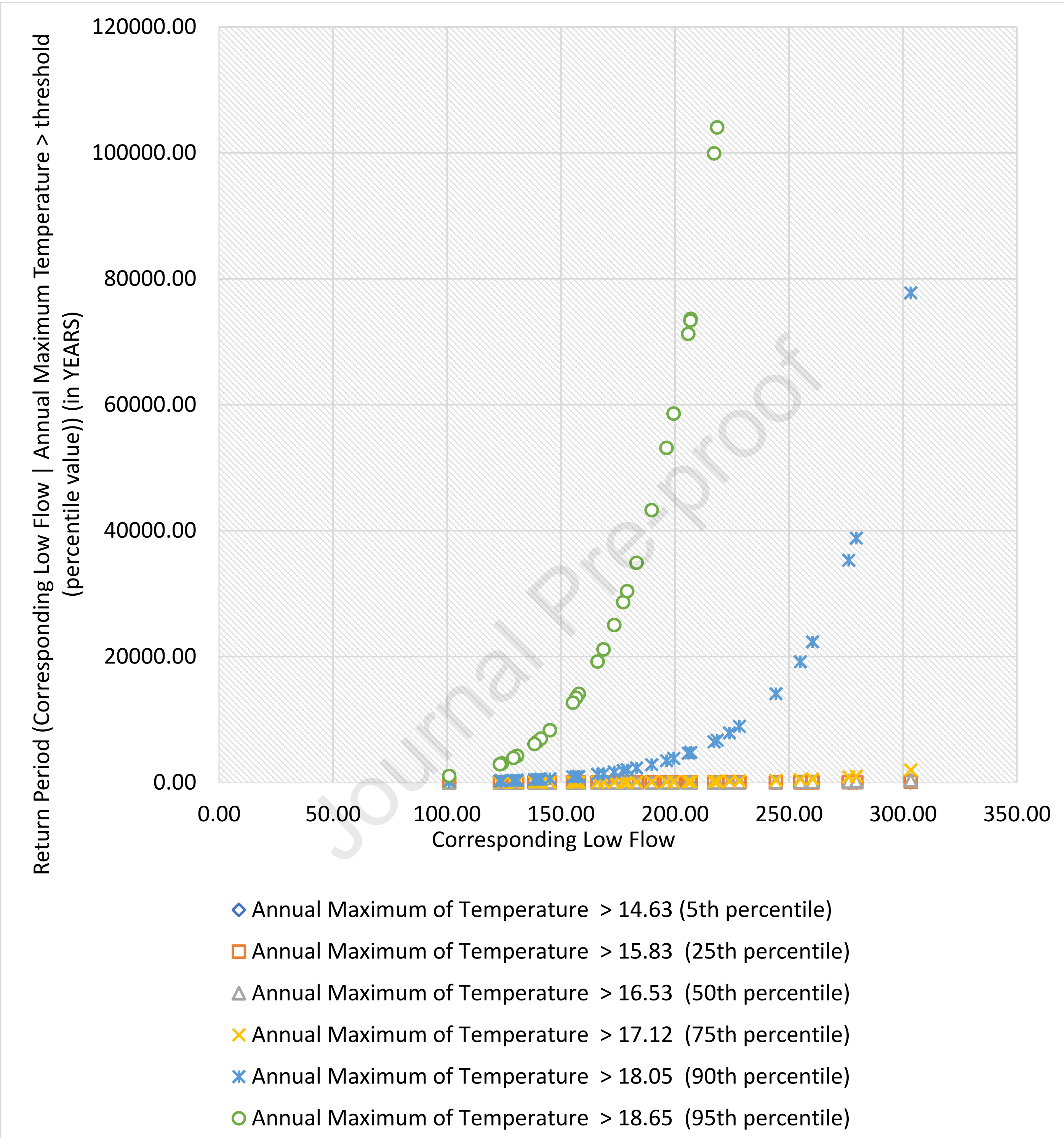

Return Period (Corresponding Low Flow | Annual Maximum Temperature > threshold (percentile value)) (in YEARS)
120000.00
100000.00
80000.00
60000.00
40000.00
20000.00
0.00
0.00
50.00
100.00
150.00
200.00
250.00
300.00
350.00
Corresponding Low Flow
Annual Maximum of Temperature > 14.63 (5th percentile)
Annual Maximum of Temperature > 15.83 (25th percentile)
Annual Maximum of Temperature > 16.53 (50th percentile)
Annual Maximum of Temperature > 17.12 (75th percentile)
Annual Maximum of Temperature > 18.05 (90th percentile)
Annual Maximum of Temperature > 18.65 (95th percentile)

(c)

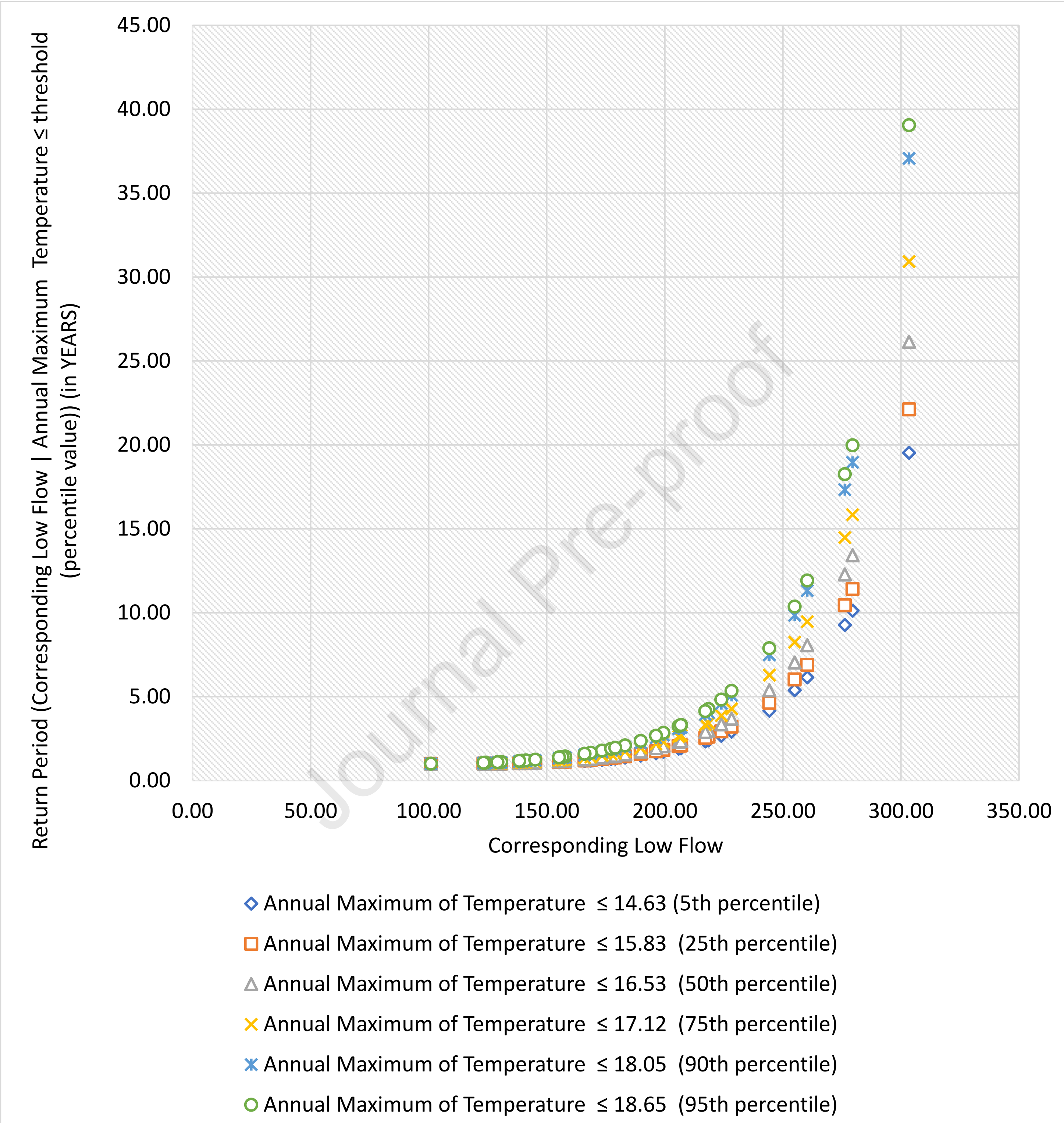

(d)

Figure 7. (a) Estimating the conditional joint return periods for station 2473 (a) for case, Annual Maximum Temperature | Corresponding Low Flow > threshold (percentile value) (b) for case,

Annual Maximum Temperature | Corresponding Low Flow ≤ threshold (percentile value) (c) for case, Corresponding Low Flow | Annual Maximum Temperature > threshold (percentile value) (d) for case, Corresponding Low Flow | Annual Maximum Temperature ≤ threshold (percentile value)).

Research Highlights

1. In Swiss Rivers, a parametric copula model was used to estimate the joint density of negatively dependent extreme river temperature and low flow.
2. Most justifiable copula densities are employed in estimating joint exceedance probability.
3. Primary for OR and AND joint cases and conditional joint return periods are estimated.
4. Simultaneous occurrences of bivariate events are less frequent in the AND-joint case than in the OR-joint event.
5. Higher return periods are observed in river temperature (or low flow) when increasing the percentile value of the conditioning variable, low flow (or river temperature).
6. Also, higher bivariate event return periods occur at higher river temperatures (or low flow) values when fixing conditioning variables (river temperature or low flow).
7. These bivariate statistics can better describe the cold-water species real risk during extreme events and help in their management.

CRediT authorship contribution statement

Shahid L: Conceptualization, Methodology, Software, Formal analysis, Validation, Writing-original draft preparation, Project administration**. Souaissi Z:** Conceptualization, Methodology, Investigation, Validation, Writing-Original draft preparation, **Taha B.M.J Ouarda:** Project Focus and Supervision, Funding acquisition, Conceptualization, Methodology, Project administration, Writing-Review & editing, Results validations**, André- St-Hilaire:** Project focus, Conceptualization, Methodology, Writing-Review & editing, Results validations.

Declaration of interests

☒ The authors declare that they have no known competing financial interests or personal relationships that could have appeared to influence the work reported in this paper.

☐ The authors declare the following financial interests/personal relationships which may be considered as potential competing interests: